ABSTRACT

Carol Elizabeth Mueller: 5-Fluorouracil: A Metabolism Model of the Rat Liver
(Under the direction of Dr. Douglas J. Crawford-Brown)

A metabolism model of 5-fluorouracil (FU), a nucleotide synthesis interference chemical, was created based on rat liver metabolism data. The model of the adult rat predicted that 0.1% of the original FU dose will become 5-fluorodeoxyuridine monophosphate (FdUMP), a thymidine synthetase inhibiting metabolite. Model parameters were derived from enzyme activity information. It can be concluded from the results of this model that a very small percentage of the initial FU dose actually becomes the metabolite FdUMP. This is the first model to focus on the anabolism portion of the overall metabolism of FU. The overall goal of the research program is to help in the develop of a pharmacokinetic, biologically based dose-response model of FU to test the feasibility for modeling nucleotide synthesis inhibitors. The rat liver metabolism is merely one part of the modeling picture which is needed to look at developmental effects due to interference with nucleotide synthesis, but it is a place to begin.

ACKNOWLEDGEMENTS

I would like to thank Dr. Woody Setzer for the pleasure of working with the EPA on this project. Many thanks to Dr. Douglas Crawford-Brown for this opportunity, as well as his guidance and direction throughout this project. I am especially grateful for his patience and encouragement. I would also like to show my appreciation to Dr. Louise Ball for the academic and personal guidance provided during my time at Chapel Hill. I extend my gratitude to the many scientists who have done research on 5-fluorouracil to provide me with the knowledge to produce this model. I would also like to thank Dr. Pauline Schwartz for her assistance and advice. Most of all, I must extend my extreme gratitude to family and friends for their understanding and support over the past year and a half.

TABLE OF CONTENTS

LIST OF TABLES

LIST OF FIGURES

LIST OF EQUATIONS

LIST OF ABBREVIATIONS

FU	5-Fluorouracil
DHFU	dihydrofluorouracil
FUPA	α-fluoro-β-ureidopropionic acid
FBAL	α-fluoro-β-alanine
BA	bile acids
CFBAL	conjugated FBAL
FA	fluoroacetate
FC	fluorocitrate
FUrd	fluorouridine
FUMP	5-fluorouridine monophosphate
FUDP	5-fluorouridine diphosphate
UDP	uridine diphosphate
CDP	cytidine diphosphate
FUTP	5-fluorouridine triphosphate
UTP	uridine triphosphate
FdUrd	5-fluorodeoxyuridine monophosphate
FdUMP	5-fluorodeoxyuridine monophosphate
dUMP	deoxyuridine monophosphate
dTMP	thymidylate
FdUDP	5-fluorodeoxyuridine diphosphate
FdUTP	5-fluorodeoxyuridine triphosphate
DPD	dihydropyrimidine dehydrogenase
TS	thymidylate synthetase
OPRTase	oratic acid phosphoribosyl transferase
PRPP	phosphoribose pyrophosphate
UP	uridine phosphorylase
R-1-P	ribose-1-phosphate
UK	uridine kinase

NDPK	nucleoside diphosphokinase
RR	ribonucleotide reductase
TP	thymidine phosphorylase
dR-1-P	deoxyribose-1-phosphate
TK	thymidine kinase
ATP	adenosine triphosphate
BBDR	Biologically based dose-response
PBPK	Physiologically-based pharmacokinetics
gd	gestation day
M-M	Michaelis-Menton

1. Introduction

1.1 Introduction to 5-fluorouracil

5-Fluorouracil (FU) was developed in 1957 as an anti-tumor drug (Parker et al. 1990). Over the years, it has become the most widely used cancer chemotherapeutic agent. It is used to treat a long list of cancers (colon, rectum, breast, stomach, pancreas, gastric, anus, bladder, cervix, endometrium, ovaries, esophagus, head & neck, penis, liver, prostate, skin, vulva) both alone and with other drugs.

The Environmental Protection Agency in North Carolina's Research Triangle Park is researching the link between FU, its metabolite 5-fluorodeoxyuridine monophosphate (FdUMP), and malformation of digits and cleft palates seen in exposed rats. FdUMP's main mode of action is the inactivation of thymidylate synthetase (TS). TS plays an important role in DNA replication in actively dividing cells (Reilly et al. 1997). A covalent inhibitory complex is formed between FdUMP, TS, and 5,10-methylene tetrahydrofolate (5,10-CH_2-FH_4) (Inaba et al. 1996). This inhibition of TS prevents the formation of nucleotides needed for DNA synthesis (Reilly et al. 1997).

FU was chosen to test the ability of models to predict the action of compounds that interfere with nucleotide synthesis, since it is one of a broad class of compounds that acts by this mechanism and there are bodies of data available on FU biokinetics, metabolism effects on TS inhibition, and consequent development effects. The overall goal of the research program is to develop a pharmacokinetic, biologically based dose-response model of FU as a test of the feasibility for modeling nucleotide synthesis inhibitors. However, according to Diasio and Harris, large gaps still remain in our knowledge of FU metabolism (Diasio et al. 1989).

Biologically based dose-response (BBDR) models are designed to improve the decisions made when assessing the health risks associated with chemical exposure. This involves creating a mathematical form which utilizes current data to investigate the

pharmacokinetics and pharmacodynamics of exposure-response relationships. The need for more developmental information has led to the creation of embryo-specific dose-response models. The ideal situation would be to have a BBDR/pharmacokinetic and metabolic model that could estimate the amount of each metabolite in all major organ systems, in both the maternal and fetal tissue.

For regulatory purposes creating a model that could be generalized to more than one species would be very beneficial. Decisions must be made to protect human health, while most models are built with data from non-human animals. A model must allow for the extrapolation to human exposure and effects if it is to be a useful tool in the risk assessment process for health effects of environmental contaminants. Therefore, the present research focuses on development of a predictive model of the metabolism of FU to FdUMP that includes all relevant metabolic steps and formulates these as differential equations whose parameters may (with adjustment for differences in enzyme concentration and activity) be extrapolated across age groups and species.

Physiologically-based pharmacokinetics (PBPK) of the translocation of FU have been modeled previously (Setzer, unpublished). The step involving FU metabolism, however, was not included. Therefore, a metabolism model of FU is needed. Once the metabolism is modeled, it can be linked to the model of translocation model, producing a complete pharmacokinetic model.

The first step in modeling FU metabolism is to focus on only one organ so metabolic steps independent of translocation may be determined. A flow chart of the modeling picture shows the role of the current research in the overall program of development of a pharmacokinetic model of FU (Figure 1). The metabolism in the rat liver is only one part of the modeling picture that is required to study the developmental effects from nucleotide synthesis interference. While the overall goal is to predict developmental effects, this project focuses on the liver metabolism in the adult, fetus, and other ages of rats.

To test the modeling of FU metabolism, the rat liver was modeled because this is where data are available and where metabolism occurs primarily. The metabolism model created using the rat liver can then be extrapolated to human liver metabolism. Eventually, what is learned will allow the modeling of the human fetus liver metabolism. Once the metabolism is linked to the model of translocation and the biologically based-dose response

models, there will be a better understanding of the causes of developmental effects from FU exposure. Before discussing the model in detail, it is important to characterize the damage seen with FU exposure, the metabolism of FU and the many different enzymes involved. Following this introduction to FU biochemistry, the mathematical model will be described.

Figure 1. Flow chart of the entire modeling picture, showing the role of the current research. Rat liver metabolism is merely one part of the modeling picture which is needed to look at developmental effects due to interference with nucleotide synthesis. Note that the overall goal is to predict development effects, and that this project contributes to that by focusing on inhibition of thymidine synthetase, then further on FU, and so on down to a focus on liver metabolism in the adult, fetus, and other ages of rats. Subsequent research may then focus on extrapolating the rat metabolic model to human liver metabolism and incorporating the metabolic model into a PBPK/BBDR model capable of predicting inhibition of TS by FU and subsequent developmental effects.

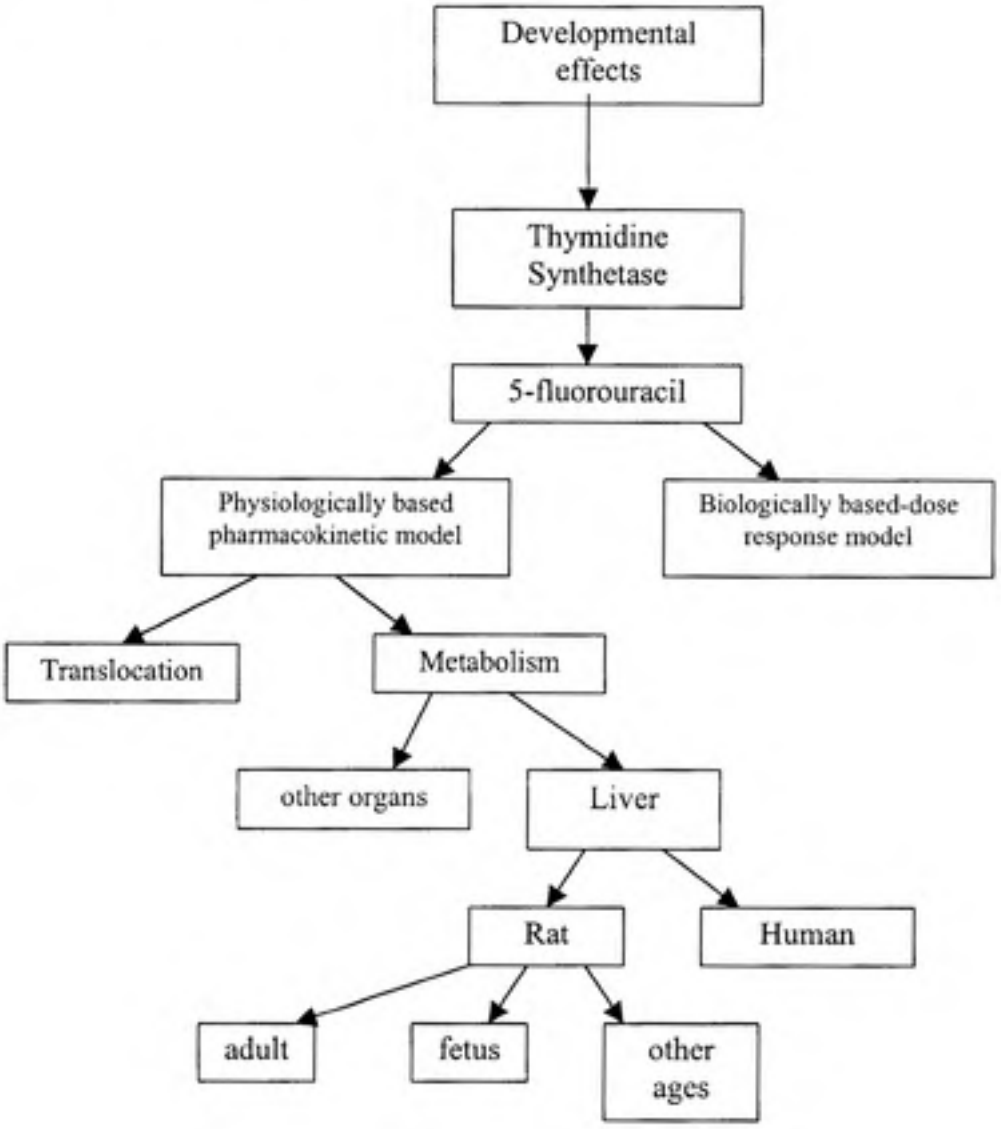

1.2 Teratogenic Information

A teratogen is defined as an agent that causes physical abnormalities in a developing embryo or fetus. Teratogens can be transported between the mother and the fetus across the placenta. The material from the maternal blood can cross the membrane and enter the fetal arterial blood (Luecke et al. 1994). It has been reported in both rats and monkeys that FU can cross the placenta using diffusion or carrier-mediated transport (Garnica et al. 1996, Toxnet). Dorko et al. (1986) discovered an increase in placental and fetal transfer of uridine as pregnancy progresses. This may also be the case with FUrd (fluorouridine).

It has been proven that FU is a teratogenic agent in the rat (Wilson et al. 1971). Depression of DNA synthesis due to thymidine synthetase inhibition by FdUMP has been measured in both maternal and embryonic tissues. When radiolabeled FU was given to pregnant rats, radioactivity was measured in the DNA and RNA of the embryos (Grafton et al. 1987). Schumacher et al. (1969) found that two-thirds of the radioactivity ends up in the RNA fraction, while very little could be found in the DNA and free protein fractions.

Fetal anemia and other organ dysfunction may contribute to the developmental toxicity of FU. Shuey et al. (1994) found that a single administration of FU on gestation day 14 in the rat will cause fetal growth retardation at maternal doses above 15 mg/kg and malformations at doses above 30 mg/kg. These same doses showed only minimal maternal toxicity. Of the external and skeletal malformations, hindlimb defects and cleft palates are the most prevalent anomalies (Shuey et al. 1994).

It has been shown in monkeys that FU has a very narrow teratogenic dose-range: that is, there is a very small difference between the no-effect level and the total embryolethal dose level. Monkey embryos were found to be able to tolerate the teratogenic dose for rats (20 mg/kg), but begin to show embryotoxicity at a one fold increase in dosage (40 mg/kg) and above (Wilson et al. 1971). No explanation has yet to be determined for this very high slope in the dose-response curve.

1.3 Neurotoxicity of FU

The FU catabolite α-fluoro-β-alanine (FBAL) has been shown to cause neurotoxicity in cats following a 30mg/kg dose of FU (Koenig et al. 1970). Akiba et al (1996) discussed the effect of FU on the central nervous system of mice with doses as small

as 10mg/kg of FBAL. They found selective white matter injury consisting of diffuse demyelination and irregular small infarcts (Akiba et al. 1996). The demyelination is often seen along with large vacuoles and gliosis in the surrounding tissue. The formation of vacuoles is due to myelin separation at the intraperiod line. This CNS problem has also been documented in human patients receiving FU chemotherapy (Akiba et al. 1996). Mice studies by Akiba et al. (1996) demonstrated that the most important issue with CNS damage is the accumulation and slow elimination of FU metabolites in the nervous system tissue, especially the myelin. It was hypothesized that FBAL and its metabolites are also responsible for the neurotoxicity in humans (Akiba et al. 1996).

Some scientists believe that FBAL is metabolized in the body to fluoroacetate (FA), a potent convulsant (Koenig et al. 1970). It is also thought that FA could be metabolically converted to fluorocitrate (FC). FC has the ability to inhibit the Krebs cycle and block aconitase, an enzyme that catalyzes the reversible interconversion of citrate and isocitrate (Koenig et al. 1970). However, Arellano et al. (1997) found that some commercial solutions of FU have impurities which come from reactions occurring in the additives needed to keep FU soluble. These impurities, fluoromalonic acid semialdehyde and fluoroacetaldehyde, are metabolized to FA and fluorohydroxypropionic acid. Therefore, it has been concluded by many that FBAL is not metabolized to FA in the body, but instead the stock solution impurities are converted to FA (Anand et al. 1994).

Zhang et al. (1992) present three possible mechanisms responsible for the neurotoxicity seen with FU: (1) the effects of an FU-nucleotide on DNA and RNA synthesis, (2) inhibition of the Krebs cycle by FC, and (3) direct toxicity of FBAL on nervous tissue. Since the Zhang et al. (1992) lab found no evidence of FC in their experimental animals, it would seem that their results agree with the thought that FC is present only when there is contamination in the FU solution.

1.4 Cardiotoxicity of FU

In addition to the neurotoxic effects, FU can also cause cardiotoxicity problems. Anand et al. (1994) present two theories to explain why FU is cardiotoxic. The first theory assumes that a complex formed with FU and cardiac cells or tissue components stimulates an autoimmune response. The second theory is that the cardiac cells are damaged by the FU

and this may cause an inflammatory response, which is then maintained by the lymphokines (Anand et al. 1994).

FBAL also accumulates in the tissues of the heart. This accumulation can interfere with taurine, a chemical that plays an important role in cardiovascular function (Zhang et al. 1993). Because of the similar chemical structures of FBAL and taurine, it is possible that the uptake and accumulation of FBAL in the heart would affect the transport and function of taurine.

1.5 Current models

Before creating a model, it is important to study models that have already been established. Models of kinetics and tissue distribution have been made for FU and its catabolites (Mentre et al. 1994, Zhang et al. 1993). So far, all of the metabolism models for FU have focused on the catabolism pathways. The nonlinear kinetics and placental transfer have been modeled in pregnant rats (Boike et al. 1989). A nonlinear pharmacokinetic model has been developed for humans (Collins et al. 1980). Biologically based dose-response models are also available (Shuey et al. 1994, Setzer et al. unpublished). No models of FU anabolism could be found in the literature.

Mentre et al. (1984) created a mathematical model based on FU catabolism in liver cells. It was developed to measure the enzymatic transformations and transmembrane exchanges involved in FU catabolism. It was written as a set of mass-balance differential equations that express rates of exchange and transformation. The model focused on the catabolic processes rather than the anabolic processes of interest in this study.

Zhang et al. (1993) developed a mathematical model to describe the kinetics and tissue distribution of FBAL in rats following an IV bolus administration of FBAL. The predictions showed an increasing transport and accumulation of FBAL in numerous tissues, many of which are associated with FBAL related toxicity. The obvious limitation of this model for the purpose of this paper is the focus on FBAL, the main catabolite.

Using pregnant rats and high-performance liquid chromatography methodology, Boike et al. (1989) reported findings on the disposition of FU. Blood samples were used to measure FU and numerous parameters were determined. However, individual metabolites

were not measured; therefore this dataset does not provide an adequate basis for estimating FdUMP amounts and possible related teratogenic effects.

Collins et al. (1980) developed a two-compartment physiologically-based pharmacokinetic model for FU in humans, incorporating saturable whole body clearance. The model predicts the disappearance kinetics after an intravenous bolus and at steady-state levels during constant intravenous infusions. Both hepatic and extrahepatic elimination were studied, but the anatomic location of the clearance was not determined. The model was also extended to include both oral and intraperitoneal administration of FU.

Shuey et al. (1994) have been working toward a BBDR model with the following framework:

1.Administered Dose ----------FU administration at gestation day 14
2.Target Dose ----------Fetal levels of FU/FdUMP (pharmacokinetics)
3.Molecular Interaction ----------Thymidine synthetase inhibition
4.Molecular Response ----------Thymidine depletion, decreased DNA synthesis
5.Cellular Response ----------Altered cell cycle
6. Tissue Response ----------Dysmorphology, growth reduction
7.Developmental toxicity ----------Fetal weight reduction, malformations

FU was used for this BBDR model as a prototype compound because its metabolism, developmental toxicity, and mechanisms of action have been well studied. Thymidine synthetase activity, cell cycle kinetics, and growth were researched over the developmental period for both the whole fetus, as well as individual embryonic tissues (Shuey et al. 1994). This model was continued in Setzer et al. (unpublished) and is based on the inhibition of thymidine synthetase and changes in the nucleotide pools, DNA synthesis, cell cycle progression, and somatic growth. Setzer et al. (unpublished) included an illustration of the proposed model that combines parameters associated with multiple metabolic steps. The resulting model is shown in Figure 2. The box containing 5-FU → 5-FdUMP is the section which is addressed and modeled in the present paper.

Figure 2. Model of 5-FU developmental toxicity by Lau et al.

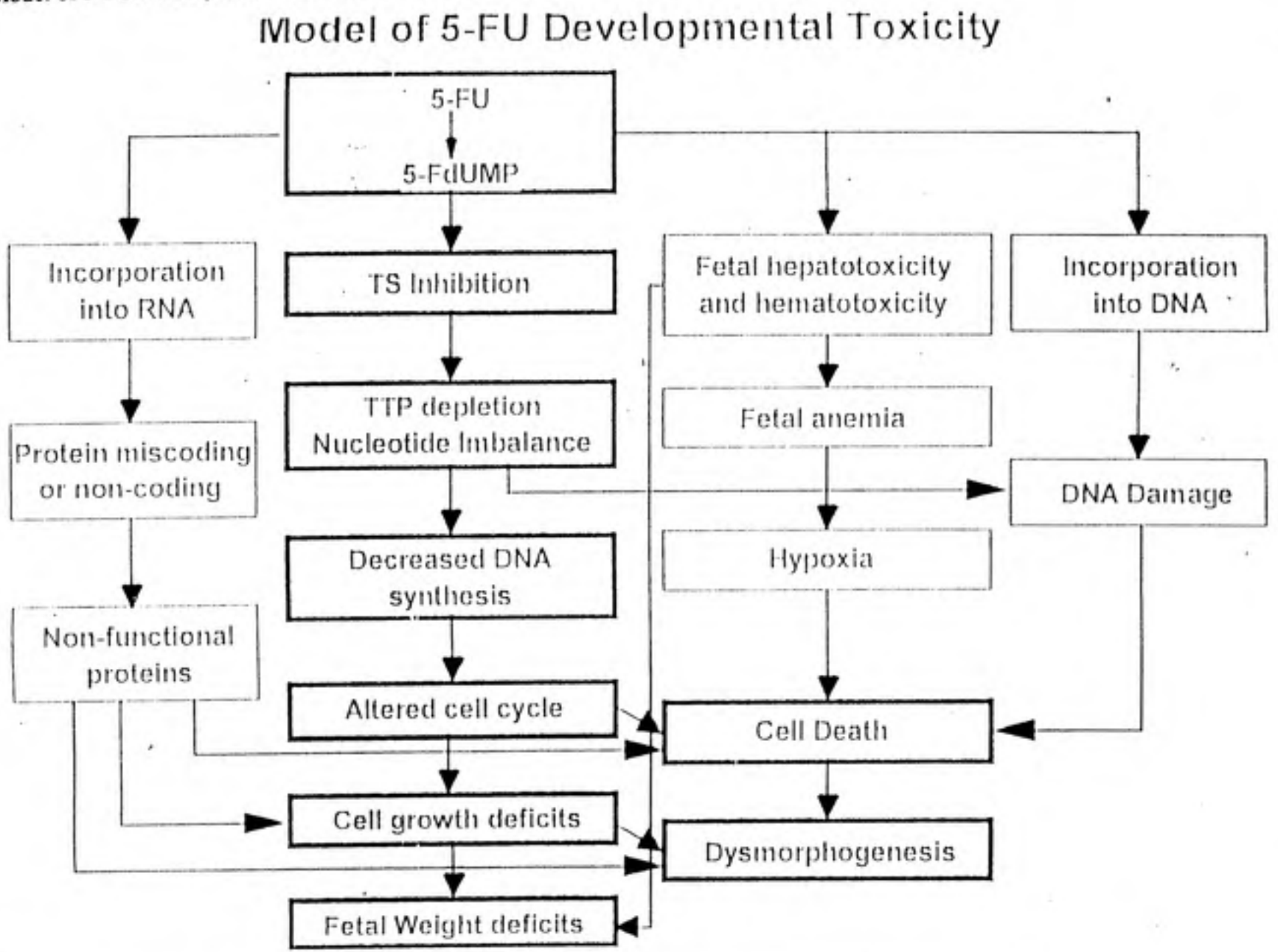

Chapter 2. 5-Fluorouracil – Metabolism and Disposition

2.1 General metabolism information

In rodents and man, FU follows a pathway similar to that of uracil both in activation and degradation (Chaudhuri et al. 1985). Unmetabolized FU has not proven to be cytotoxic (McSheehy et al. 1997). Clinical studies show FU can be distributed throughout the body, including extracellular space, as well as into most tissues (Diasio et al. 1989). According to TOXNET, FU easily crosses the blood-brain barrier and placenta-fetal barrier. The amount of FU available for anabolism is determined by the amount of catabolism which can take place (Diasio et al. 1989). The two pathways are competing for each FU molecule. A flow chart was compiled for the present study using available data to create a conceptual model of fluorouracil metabolism (Figure 3).

The liver is the primary site of metabolic activity. However, a catabolic and anabolic pathway has been measured outside the liver (Barberi-Heyob et al. 1995). Elimination of FU by isolated rat liver cells follows Michaelis-Menton kinetics, in which the initial phase of zero-order elimination occurs at concentrations above 100μM, and is followed by a first-order elimination phase at low concentrations (LaCreta et al. 1989). The rate of elimination of FU in plasma of rats was observed to be dose-dependent when FU is given by IV injection (Schwartz et al. 1985).

Clearance has been quantified by a ratio of the rate of elimination of a chemical from an appropriate reference fluid, usually plasma, to its concentration in that same fluid. The resulting ratio is a measure of the efficiency of the overall removal of the chemical from the body (i.e. of the first-order rate constant for removal). Total system clearance is the sum of the clearances by individual pathways. The presence of extrahepatic metabolism is to be expected since the total system clearance of FU is higher than the hepatic blood flow (Barberi-Heyob et al. 1995). Renal clearance of FU and its metabolites was found to be approximately 10 to 15% of the total FU clearance in humans (Joulia et al. 1997). The Kao et al. (1985) pharmacokinetic studies of FU in rats also demonstrated that the non-renal

clearance was higher than the hepatic blood flow, thus indicating possible extrahepatic routes of FU elimination (Kuan et al. 1998).

The individual importance of each of the possible extrahepatic routes has not yet been quantified. However, a few of the possibilities have been studied (Kao et al. 1985, Kuan et al. 1998). The pulmonary route was considered as a possible extrahepatic pathway due to its known influence on drug elimination (Kao et al. 1985). When doing pulmonary extraction measurements of FU, the dog shows results similar to humans. Pulmonary clearance can be substantial at low doses. This is especially true with dogs because of their large lung perfusion rates. In the lungs, the FU metabolism was determined as a rapidly saturable pathway. The gastrointestinal tract was also determined to be a saturable pathway for FU metabolism (Kuan et al. 1998).

Figure 3. Flow chart of 5-Fluorouracil metabolism

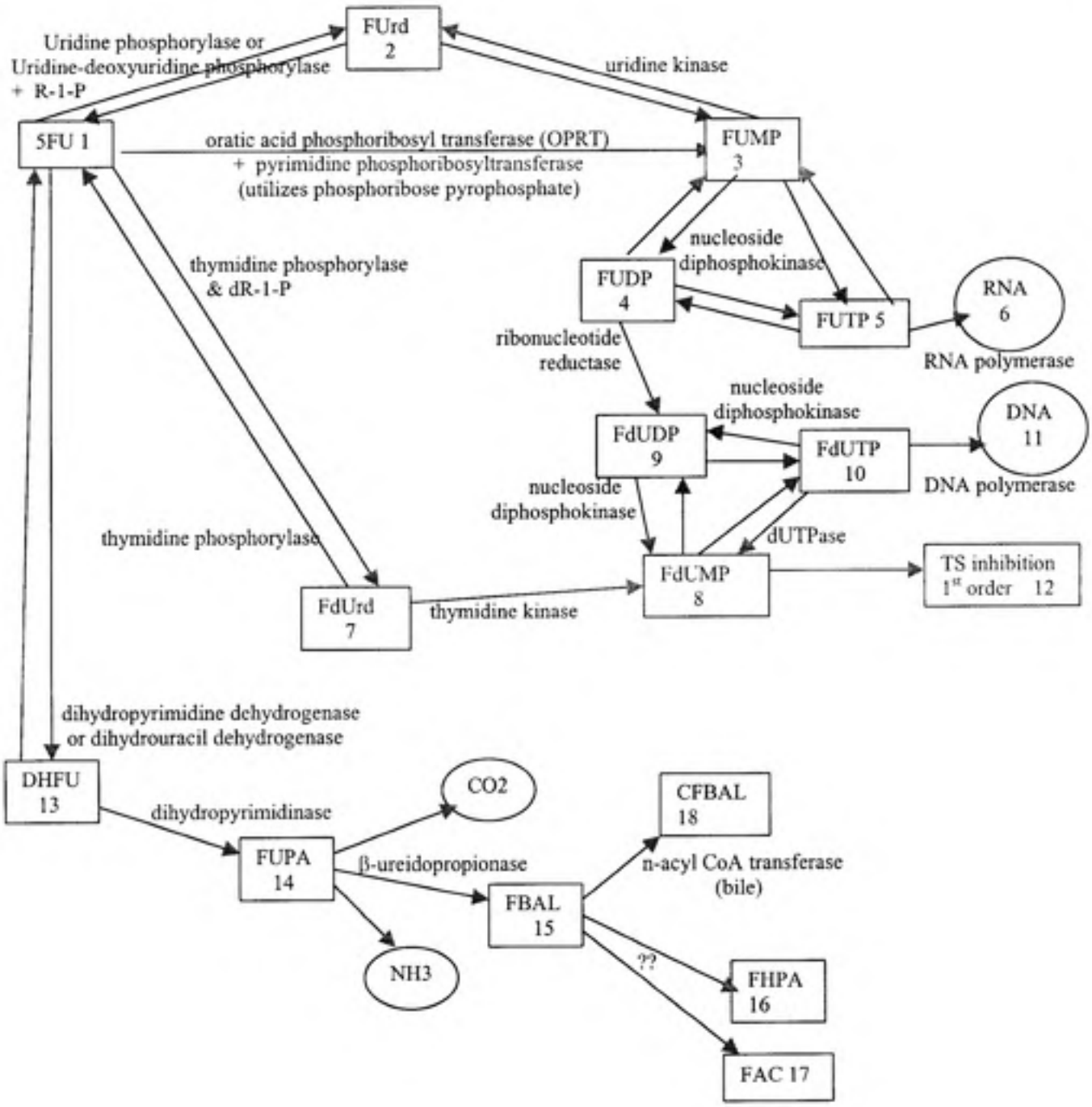

2.2 Catabolism of 5-Fluorouracil

Elimination of FU occurs through two major routes: (1) renal clearance of the unchanged drug and (2) catabolic breakdown, most occurring in the liver. The end products of FU catabolism, α-fluoro-β-ureidopropionic acid (FUPA) and FBAL, are removed by the kidneys (Barberi-Heyob et al. 1995). The removal of FU in its unchanged form, FBAL, and FUPA usually occurs through the urine within 6 hours of drug administration (Ardalan et al. 1998). The effect of the catabolic pathway is to rapidly breakdown FU to FBAL, an amino acid metabolite, and reduce the bioavailability of the FU for activation (Kissel et al. 1997).

A significant correlation was discovered between the clearance of FU and the activity of the enzyme DPD (dihydropyrimidine dehydrogenase). DPD activity is the rate-limiting step of the catabolism of FU (Barberi-Heyob et al. 1995). It is found in most normal and neoplastic tissues, while the highest amounts are found in liver cells (Horowitz et al. 1995, Kissel et al. 1997). When laboratory rats were denied protein, the amount of DPD activity decreased (Roos et al. 1997). High DPD activity in the liver results in a rapid degradation of FU. The activity of DPD in the rat liver is in the same range as the human liver (Peters et al. 1998). The activity level of DPD fluctuates in a circadian rhythm creating a mirror image oscillation of plasma FU concentration during constant exposure (Khor et al. 1997).

DPD is involved in the first step in FU degradation. It occurs through the reduction of the pyrimidine ring that converts FU to DHFU (dihydrofluorouracil) (Ardalan et al. 1998). It is very important to realize that this reaction is the reversible reduction of FU (Naguib et al. 1985). This reaction is considered unusual since it is a catabolism reaction with NADPH as the reductant. However, the ratio of NADPH/NADP+ exceeds that of NADH/NAD+ in the cells. This is one reason why most cells favor catabolism (Rosksoski, 1996).

The remaining steps of catabolism are rather simple. DHFU is converted to FUPA in a hydrolysis reaction. This catabolite can be excreted in the urine (McSheehy et al. 1997). FUPA can be metabolized further to FBAL, with by-products of CO_2 and NH_3 (Horowitz et al. 1995). β-ureidopropionase is the enzyme responsible for the irreversible transformation of FUPA to FBAL through hydrolysis (Naguib et al. 1985).

FBAL is the main catabolite for both humans and experimental animals, and is mainly excreted through the kidneys (McSheehy et al. 1997). Urine is the major pathway in rats, while fecal elimination is a minor pathway excreting less than 10% of the administered

dose in this manner. Tissue distribution of FBAL includes the enterohepatic, nervous, and muscular systems. When radiolabeled FBAL was injected into rats, radioactivity accumulated and remained longer in tissues such as the liver, intestines, brain, heart, and skeletal muscles. Pharmacokinetic analysis of FBAL in the plasma of rats demonstrated that it has a prolonged elimination half-life, and is often described as having 2 short half-lives and one prolonged half-life. The first two half-lives illustrate FBAL being distributed into well perfused tissues including the liver, kidneys, heart, lungs, and spleen. The third phase is evidence of the retention of FBAL and its metabolites in tissues such as the liver, intestine, brain, heart, and skeletal muscle. Given all of this evidence and the toxicity information from the previous sections, FBAL must play a major role in the hepatobiliary toxicity, neurotoxicity, and cardiotoxicity of FU (Zhang et al. 1992).

FBAL can be conjugated with bile acids (BA) in the place of taurine and glycine by n-acyl CoA transferase, making CFBAL (conjugated FBAL) the major biliary metabolite of FU (Diasio et al. 1989). The FBAL bile acids formed in rats include FBAL-cholate, FBAL-chenodeoxyxholate, and FBAL-muricholate. FBAL-BA conjugates undergo an enterohepatic circulation with deconjugation in the intestines and reconjugation in the liver (Zhang et al. 1992).

2.3 Anabolism of 5-Fluorouracil

The anabolic pathways of FU are basically the same as the *de novo* pathways of uracil (Diasio et al. 1989). The type of damage resulting from FU exposure depends upon metabolic activation of FU to a nucleotide (Schwartz et al. 1985). Each tissue can experience a different response from FU depending on the activity of the important enzymes in that tissue. Because the metabolism takes place within the cells, blood levels of FU cannot accurately reflect the levels of anabolites in the tissues. Unfortunately, this makes blood, along with most other biological fluids, a very poor indicator of FU anabolite levels (Barberi-Heyob et al. 1995).

It is assumed that most bioactivation of drugs and chemicals would occur in the maternal liver (Juchau et al. 1989). However, a majority of the reactive intermediates generated in the maternal liver would have a difficult time reaching the fetus due to their reactivity and short half-lives (Juchau et al. 1989). The following must happen before a

reactive material reaches the fetal cells: exportation from hepatocytes in maternal liver, transportation through the maternal blood stream, passage across the chorioallantoic and/or yolk sac membranes, and transportation into the fetal circulation. Therefore, some researchers have concluded that only stable and low reactivity metabolites would reach the fetus (Juchau et al. 1989).

Another possible explanation for the fetal developmental effects is that FU is metabolized within the fetus itself. On gestation day 11 (gd11), the embryo has negligible ability to degrade FU (Schumacher et al. 1969). Yet late in gestation, the fetal liver is developing blood cells in the vicinity of hepatocytes that are metabolizing nutrients. These hepatocytes have the ability to metabolize chemicals and drugs to an active form (Cole et al. 1979). An anabolic environment is present in a growing fetus creating a uni-directional flow of metabolism (Beckman et al. 1996). The kinase needed for FU phosphorylation is present in the embryo at gd11 and its activity level is 15 to 20 times higher than in maternal liver homogenate (Schumacher et al. 1969).

As mentioned above, the initial step of metabolism is determined by the amount of FU that is available for anabolism, since catabolism and anabolism compete for FU (Diasio et al. 1989). Each FU molecule can theoretically go in one of four directions:

1. FU can become deactivated directly through DPD activity.
2. FU can go directly to FUMP, with FdUMP as a final product
3. Use the de novo pathway to get to FUMP in 2 steps, with FdUMP as a final product
4. FU can become FdUMP in 2 steps.

2.3.1 5-fluorouridine monophosphate

The direct pathway for FU to become FUMP (5-fluorouridine monophosphate) is catalyzed by oratic acid phosphoribosyl transferase (OPRTase) and its utilization of phosphoribose pyrophosphate (PRPP). OPRTase was initially discovered by Lieberman et al. in 1955. It is widely distributed in the body of mammals (Reyes et al. 1975). The OPRTase activity is the rate limiting component for this direct conversion (Peters et al. 1986). Higher activity of OPRTase is present in the rat liver than exists in the intestinal

mucosa cells (Raisonnier et al. 1981). PRPP is a common substrate for synthesis of purine, pyrimidine, and pyridine ribonucleotides (Hisata et al. 1975).

The *de novo* pathway to FUMP has two steps. The first step is 5-fluorouridine (FUrd) formation. This involves ribosylation of FU initiated by the enzyme uridine phosphorylase (UP) and co-substrate ribose-1-phosphate (R-1-P). It is an essential metabolite for this "salvage" biosynthesis. R-1-P is present at high levels in mammalian cells (Cappiello et al. 1998). When rat tissues were measured, the R-1-P level was highest in the liver, followed by the brain, kidney, skeletal muscle, and spleen (Ipata et al. 1981).

In normal cell lines UP is part of the plasma membrane (Bose et al. 1977). When cells showed low FU sensitivity they often had a very low UP activity level (Peters et al. 1986). UP is found in the nuclei of nonparenchymal cells, but not hepatocytes, while the highest levels of activity were attributed to the Kupffer cells (Liu et al. 1998). There was no activity found in lysosomes or associated with mitochondria (Bose et al. 1977). In addition, rodent tissues have been found to have higher UP activity than human tissues (Meahara et al. 1989). UP has proven to play a significant role in phosphorylation in the mouse liver, but not in the human liver (el Kouni et al. 1993).

The second step in this pathway is catalyzed by uridine kinase (UK), which is present in most tissues (Schwartz et al. 1985). UK has been recorded to have a close correlation with tissue growth rates in rats. UK levels seem to be both tissue-specific and age-dependent. In both adult and fetal rat tissues there is a wide distribution of UK. UK activity is centered in the cytosolic fraction in the adult rat liver, kidney, and lung, and fetal liver and lung. Enzyme activity is highest in tissues with continuous cell production (Herzfeld et al. 1979).

In the rat, the forms and levels of activity of uridine kinase change over development and birth until they stabilize in adulthood. A change in the amount of enzyme present in the liver, lung, small intestine, and pancreas occurs over time. In the liver, the soluble fraction of UK decreases at the end of gestation only to rise after birth. At three days after birth, the UK level is 3 times the normal adult amount. The periods of maximum UK activity in the liver coincide with the time when several amino acid-metabolizing enzymes are also at their highest activity. The amino acid-metabolizing enzymes include aspartate aminotransferase, glutamate dehydrogenase, and pyroline-5-carboxylate reductase. The rat lung UK activity increases both in the soluble fraction and in the particle-bound UK after birth. The kidney

UK activity rises to 180% of the adult level in the first week after birth. The rat brain has the highest UK activity in the late gestation period, and also has high activity through the suckling period. It is interesting to note that the UK activities in the rat liver, lung, kidney, and brain never are below the level found in homologous adult rat tissues (Herzfeld et al. 1979).

The fetal rat liver has four different forms of UK, titled types I-IV. Type I is present in the rat liver up through the 20th day of gestation. Type II can be found up to the 3rd or 4th postnatal day. An adult pattern of UK is seen in the rat by postnatal day 5. Type-I is never found in adult tissue. The adult kidney is the only organ or tissue type that contains types II-IV of UK. The spleen and the liver contain both type III and IV, but type IV is scarce in the liver. The cerebrum contains type IV (Absil et al. 1980).

2.3.2 5-fluorouridine diphosphate

FUDP (5-fluorouridine diphosphate) is formed from FUMP in a reaction catalyzed by nucleoside diphosphokinase.

$$ATP\ (2\sim) + UMP\ (0\sim) \Leftrightarrow ADP\ (1\sim) + UDP\ (1\sim)$$

The ~ is the notation for a high energy bond. The number of high energy bonds remains the same on both sides of the equation. Nucleoside diphosphosphate kinase (NDPK) mediates the phosphorylation of nucleoside monophosphates. It is an enzyme with a broad specificity allowing it to catalyze the phosphorylation of the diphosphates also.

$$ATP\ (2\sim) + UDP\ (1\sim) \Leftrightarrow ADP(1\sim) + UTP\ (2\sim)$$

Again, the number of high energy bonds remains the same. It has also been discovered that this enzyme requires magnesium ions to perform phosphorylation of nucleoside monophosphates and diphosphates because the substrates and products are metal-nucleotide complexes (Rosksoski, 1996).

FUDP can be converted to FdUMP through the action of ribonucleotide reductase (RR). Ribonucleotides are converted to deoxyribonucleotides by replacing the hydroxyl

group with a hydrogen. In this case, FUDP is the substrate for RR. The reaction catalyzed by this enzyme involves the reduction of thioredoxin and the ribonucleotide. This results in a deoxyribonucleotide, an oxidized thioredoxin, and water. Thioredoxin is a protein with two cysteines which are separated by one residue in the primary structure. The reduction of FUDP by thioredoxin is irreversible (Rosksoski, 1996). The reduction of FUDP to a deoxyribonucleotide requires the activation of RR by adenosine triphosphate (ATP). Measurements indicate that the reduction of UDP requires activation by 1 to 2 mM of ATP (Moore et al. 1966).

With a pool of deoxyribonucleotides in mammalian cells that is inadequate to support DNA synthesis for more than a few minutes, deoxyribonucleotide synthesis must occur rapidly to promote DNA synthesis in cell replication. The specific activity of ribonucleotide reductase is closely related to cellular proliferation. This was demonstrated in the liver when the specific activity of the enzyme increases during liver regeneration and the DNA-synthetic period of the cell cycle. The changes in activity may be due to de novo enzyme synthesis rather than an increase in enzyme activation. An increase of reductase activity by 60% has been recorded in rats receiving FU treatment (Elford et al. 1977).

The formation of deoxyribonucleotides by RR is a very complex reaction, having multiple receptor sites and multiple feedback effects. The effects of substrates and effectors have been experimentally observed on the rate of RR reactions (Jackson, 1989). For example, dATP is a feedback inhibitor of RR activity. However, the feedback effects do not regulate the overall RR reaction rate, it is regulated by the total amount of RR present (or Vmax) (Jackson, 1989). For the purposes of this metabolism model, the reactions involving RR were greatly simplified.

2.3.3 5-fluorouridine triphosphate

FUTP (5-fluorouridine triphosphate) can be formed when nucleoside diphosphokinase assists the conversion from FUMP. Phosphorylation of FUDP can also create FUTP. The phosphorylation of FUDP to FUTP is considered a substrate-level phosphorylation, the generation of an energy-rich phosphate bond driven by the breakdown of a more energy-rich substrate. FUTP competes with the natural substrate UTP for incorporation into RNA (Peters et al. 1986). If FUTP is incorporated into RNA, it can cause

disruptions of future RNA and protein synthesis (McSheehy et al. 1997). Thus, FUTP causes alterations in both the process and functional aspects of RNA (Stevens et al. 1984). The RNA-directed effect has been classified as exerting a cell cycle phase-nonspecific action when exposure duration to the cells is short (Inaba et al. 1996).

Lokich et al. (1998) suggested that FU is incorporated into RNA not to damage the function of RNA, but rather to prolong the availability of FU for FdUMP-mediated TS blockage. Therefore, FU is not available for elimination because it has been incorporated into RNA in the place of uracil. However, it can be removed from RNA by repair mechanisms become available for metabolism to FdUMP. This affects the pharmacokinetics by creating a reservoir of FU within RNA. However, RNA does not have a very long life so this reservoir may not be an issue in developmental effects.

2.3.4 5-fluorodeoxyuridine monophosphate

FU can also be metabolized to FdUrd (5-fluorodeoxyuridine monophosphate) by ribosylation initiated by the enzyme thymidine phosphorylase and co-substrate deoxyribose-1-phosphate (dR-1-P) utilizing ATP as the phosphate donor (Laskin et al. 1979). Thymidine phosphorylase (TP) is widely distributed in normal and tumor cells (Cappiello et al. 1998). While the rat spleen has low TP activity levels, the human spleen shows very high levels of TP activity (Liermann et al. 1984). The human liver has the highest TP activity, followed by the human placenta, with the mouse liver having the lowest (el Kouni et al. 1993). FdUrd can be taken into cells rapidly. Here it is either converted back to FU or it continues toward FdUMP (Naser-Hijazi et al. 1991). The process where FdUrd reacts with a phosphate to form FU and dR-1-P is catalyzed by thymidine phosphorylase (LaCreta et al. 1989). This occurs rather quickly when sufficient ATP is present (Peters et al. 1986). Because the phosphorylase activity in the liver and most normal tissues is 2 to 3 orders of magnitude higher than the kinase, FdUrd is rapidly converted to FU (Naser-Hijazi et al. 1991).

FdUrd is a precursor to FdUMP (5-fluorodeoxyuridine monophosphate). Thymidine kinase (TK) initiates the conversion of FdUrd to FdUMP. This pathway has been shown to be of very little importance in the metabolism of FU. The low level of dR-1-P makes this pathway almost nonfunctional even if the amount of TP present is high (Inaba et al. 1996). When FU is given with deoxyinosine, a dR-1-P donor, ample FdUMP is formed in all cells

(Laskin et al. 1979). FdUMP can also be formed from the reduction of FUDP by ribonucleotide reductase to FdUDP, which is then dephosphorylated to FdUMP (Peters et al. 1986). A decreased production in FUMP can affect the level of FUDP, FUTP, and FdUMP (Inaba et al. 1996).

FdUMP's main mode of action is the inactivation of thymidylate synthetase (TS). TS plays an important role in DNA replication in actively dividing cells (Reilly et al. 1997). It is an enzyme that catalyzes the methylation of dUMP (deoxyuridine monophosphate) to form thymidylate (dTMP). The rate of inactivation depends on the concentration of dUMP present (Myers et al. 1981). A covalent inhibitory complex is formed with FdUMP, TS, and 5,10-methylene tetrahydrofolate (5,10-CH_2-FH_4) (Inaba et al. 1996). This complex inhibits the formation of the DNA precursor dTTP (Ardalan et al. 1998). The inhibition of TS brings on an intracellular increase in the dUMP pools (Rustum et al. 1997). The inhibition rate and the stability of the complex are dependent upon the amount of enzyme present. The cellular concentrations of 5,10-methylene tetrahydrofolate, dUMP, and FdUMP also have an affect on TS inhibition (Barberi-Heyob et al. 1995).

2.3.5 5-fluorodeoxyuridine diphosphate and 5-fluorodeoxyuridine triphosphate

FUDP can become FdUDP (5-fluorodeoxyuridine diphosphate) through a reaction with the enzyme ribonucleotide reductase. FdUMP can also be converted to FdUDP catalyzed by nucleoside diphosphokinase. Both FdUMP and FdUDP can be converted to FdUTP (5-fluorodeoxyuridine triphosphate). FdUTP can act as a substrate for α-DNA polymerase (Hamada et al. 1996). A decrease in dTTP pools can allow FdUTP incorporation leading to inhibition of DNA chain elongation (Ardalan et al. 1998). This misincorporation can cause toxic single and double-strand DNA breaks (McSheehy et al. 1997). Uracil-DNA glycosylase can remove the FdUTP incorporated into the DNA (Hamada et al. 1996). With sufficient FdUTP incorporation, the repair process may only damage the structure of the DNA leading to the strand breaks (Diasio et al. 1989). The enzyme dUTPase hydrolyzes FdUTP back to FdUMP and 2 phosphates quickly to prevent incorporation into DNA. Thus, if any FdUTP is detected there must be an excess of dUTP present to occupy the dUTPase enzyme (Hamada et al. 1996).

2.3.6 Similarities and differences between human and rodent 5-FU metabolism

It has been reported that the bioavailability and host-toxicity of FU follows a circadian rhythm in rodents and humans. The enzymes OPRTase, UP, and DPD, but not TP, show a change that follows a circadian rhythm. In addition, plasma uridine concentrations also follow a circadian rhythm, and it is the inverse of the UP activity (Naguib et al. 1993).

Humans and rats are quite different when considering both the amount of enzyme present and their activity levels. In rats, the activities of UP and UK, as well as OPRTase, are high in the liver, while TP and TK have a minor role in FU conversion (Maehara et al. 1989). The function of the UP/UK pathway and the OPRTase pathway are almost equal in rats. In the human liver, TP and TK are as important as UP and UK in FU phosphorylation. The OPRTase pathway plays a very small part in FU phosphorylation in humans. The main pyrimidine nucleoside phosphorylase in humans is TP (Maehara et al. 1989). UP and TP activities exhibited inter- and intra-species differences (el Kouni et al. 1993). All of these findings illustrate the importance of using human data to determine which pathways are most influential on the toxicity and chemotherapeutic ability of FU in humans (el Kouni et al. 1993). The present research, therefore, focuses only on development and parameterization of a model of FU metabolism in the rat, and not on extrapolation of the model to humans.

2.4 Fluorouracil Metabolism Model

The goal of this research was to create a mathematical model of the metabolism of FU in the rat to link to the physiologically-based pharmacokinetic model being developed by the EPA (Setzer, unpublished). The EPA FU model currently does not reflect metabolism when determining the amount of metabolite present that can cause damage, using instead the predicted FU concentration as a surrogate for metabolite dose. The model presented in this paper is focused only on the metabolism of 5-fluorouracil in the rat liver as described in the earlier chapter, dealing primarily with the anabolic portion. It consists of a group of chemical compartments that represent the parent compound as well as the different metabolites discussed in section 2.3, which are related to the routes of metabolism that lead to FdUMP. The model was created following a mass-balance approach using differential equations, in which the rate of change of a metabolite in an organ (liver) equals the difference between the rate of production of the metabolite and its rate of destruction.

Translocation between tissues is not considered, so only data in which translocation is insignificant were utilized in developing metabolic parameters.

2.4.1 Transformation Kinetics

Rates of transformation between compounds are represented in the model by first-order kinetics. It is plausible that the actual reactions involved in the elimination of FU in the liver are governed by more complex kinetics, principally Michaelis-Menton kinetics. In fact, this is likely to occur at sufficiently high concentrations. LaCreta et al. (1989) demonstrated that there is an initial phase of zero-order elimination that occurs when the concentration of FU is above 100μM, and is followed by a first-order elimination phase at concentrations lower than 100μM. Most of the measurements used in the current study were conducted at concentrations at or near the region of first order kinetics (this issue is discussed later in more detail).

The curve in Figure 4 illustrates the decision to assume first-order kinetics. The relationship between concentration and reaction velocity (rate of generation of product) is shown in Figure 4. Saturation of the enzyme system results in saturation of the reaction rate, with increasing concentration of FU. Note in Figure 4 that the reaction velocity (rate of production of the metabolic product) is first-order at low concentrations of FU but becomes zeroth order at higher concentrations due to saturation of the enzyme system. This is the classical appearance of reaction curves under Michaelis-Menton kinetics. If we assume the experiments are conducted at sufficiently low concentrations to avoid saturation, then the reaction is governed by first-order kinetics at all concentrations of FU. The governing differential equation then is:

(1) Velocity of reaction = rate constant x FU concentration

or

(2) Rate constant = Velocity of reaction / FU concentration

The theory of Michaelis-Menton (M-M) kinetics states that the dissociation rate is low compared to the rates of formation and redissociation of the enzyme-substrate complex (Matthews, 1990). Additional information is required before it is clear that a process follows M-M kinetics; usually it must be established that steady state or equilibrium conditions apply.

$$E + S \Leftrightarrow ES^* \Leftrightarrow E + P$$

E is the enzyme involved, S is the substrate, and P is the product formed. ES* represents the enzyme-substrate complex. Using this theory, the M-M equations is as follows:

(3) $$V = \frac{[S] \times Vmax}{[S] + Km}$$

Vmax, or the maximum reaction velocity, is approached at high substrate concentrations. This occurs because the enzyme molecules become saturated. Therefore, every enzyme molecule is occupied with a substrate and carrying out the catalytic step. Km is the equilibrium constant for dissociation and equals the substrate concentration [S] at which V equals ½ Vmax. Km is associated with the strength of binding of the substrate to the enzyme.

$$(E + S \Leftrightarrow ES)$$

When [S] is large, the reaction velocity approaches the value of Vmax. In a situation where the substrate is present in very low concentrations, that is, [S] is much less than Km, then most of the enzyme is free. Then first order kinetics apply, approximately, and the reaction rate becomes:

$$V = Vmax\ [S] / Km$$

From Equation (1), it may be seen that Vmax/Km equals the first order rate constant.

Only one of the studies used for determining the rate constants for the present model was conducted at an FU concentration initially above 100μM {the Schwartz et al. study

(1985) had an initial FU concentration of 200μM}. Since the reactions being studied in this paper occur quickly, the concentration in even the Schwartz et al study may be expected to drop below 100μM after the first few minutes and would then be in the first-order elimination phase for the remainder of the reaction time (during which most of the metabolic measurements were performed). Readings in that study were taken 30 minutes to 3 hours after the initial exposure, so the measured reaction rates represent the region between first order kinetics (where Equation 1 applies) and saturated kinetics. As a first approximation, first order kinetics will be assumed here, and the potential effects of this approximation assessed.

The model presented in this paper could be converted to use M-M kinetics, and not first order kinetics. The equation for the rate would change from the first order assumption:

$$\text{Rate} = \lambda \times [S]$$

To use M-M kinetics, the rate equation would be changed to:

$$\text{Rate} = \frac{[S] \times Vmax}{[S] + Km}$$

2.4.2 5-FU Model

A biologically-based metabolism model was created with FU as the input and FdUMP as the major endpoint. A graphical depiction of the structure of the model is displayed in Figure 5. Each box (compartment) represents FU or one of its metabolites. The connecting arrows between boxes represent the rate at which the component in the starting box is enzymatically converted to the component in the ending box. The circles unconnected to arrows are the rate constants for metabolism associated with the different metabolic pathways. This figure is essentially the same as the conceptual model in Figure 2. The sole difference is that some of the reversible pathways in Figure 2 cannot be modeled independently due to a lack of data (i.e. the forward and backward reactions cannot be determined independently), and so only the net rate of flow is shown in Figure 5. Both the

forward and the backward reaction outcomes were measured for only one pathway (Schwartz et al. 1985).

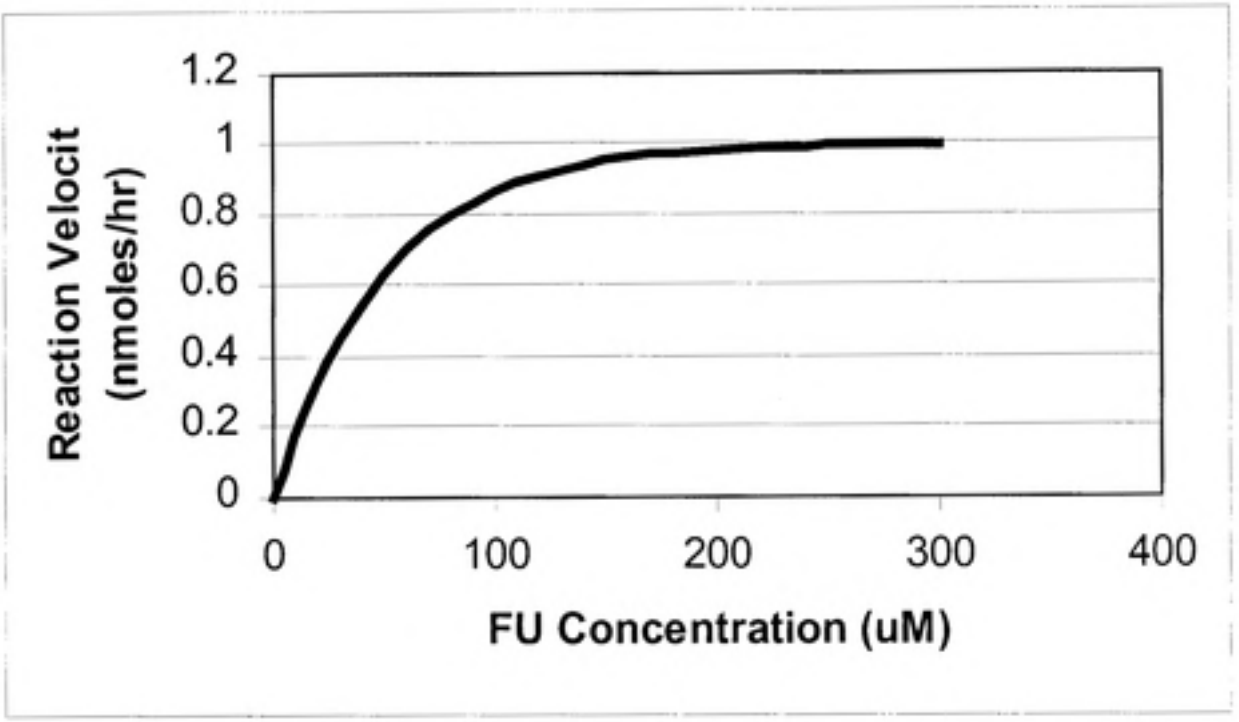

Figure 4. A theoretical representation of the change in reaction velocity with increasing FU concentration, illustrating the change from first-order kinetics at FU concentrations below 100μM to zero-order kinetics at FU concentrations greater than 100μM.

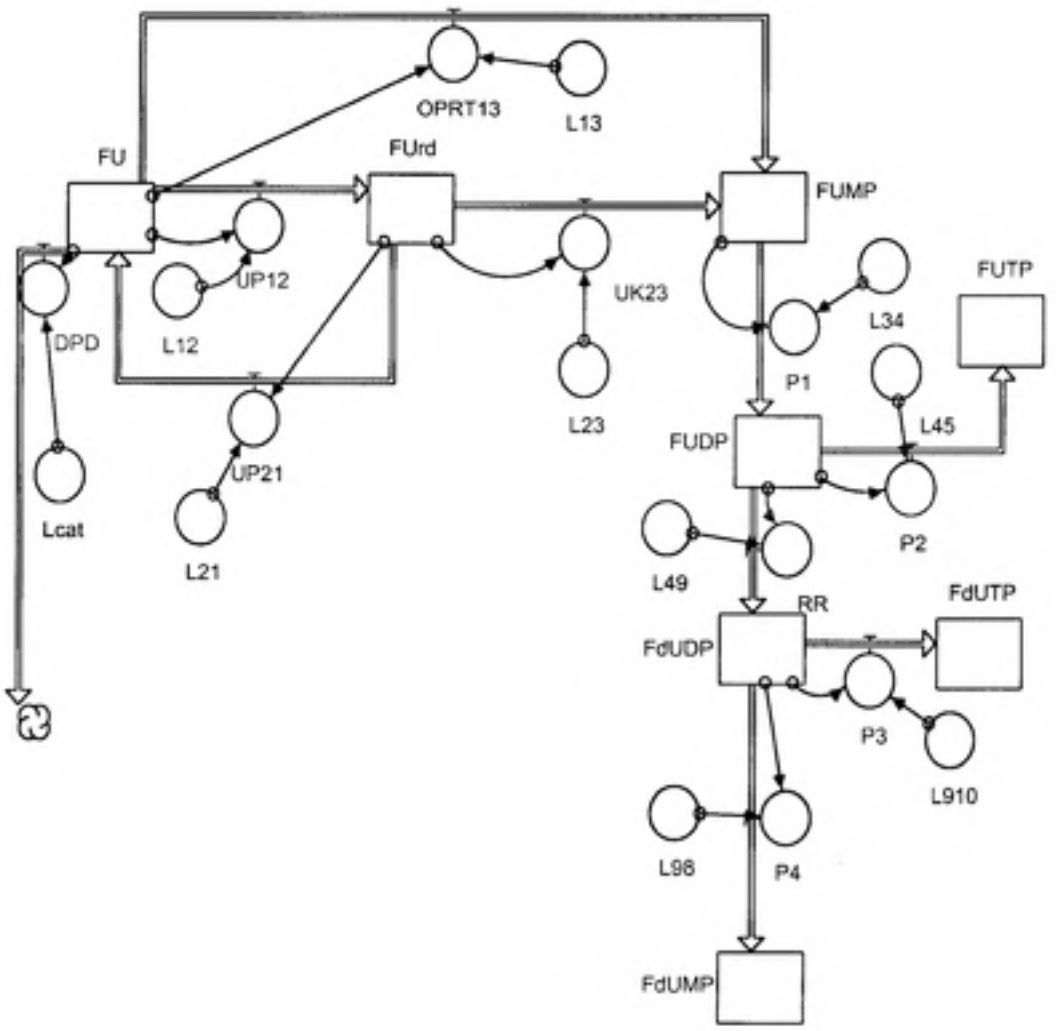

Figure 5. Stella model of 5-fluorouracil metabolism in the isolated rat liver focusing on the anabolism pathways where each compartment (box) represents FU or one of its metabolites and the arrows represent the enzymatic process which occurs between two compartments. The L is the lambda value or first order transformation rate constant for the enzymatic process between two compartments. P represents the enzyme nucleoside diphosphokinase.

2.4.3 Rate Constants and Differential Equations

The amount of FU or metabolite was calculated by the following general form of differential equation:

(4) $$dN_i(t) = [\Sigma \lambda_{ji} N_j(t) - \Sigma \lambda_{ij} N_i(t)]\, dt$$

where:

- N_i in the amount of the component (FU or metabolite) represented by compartment 1 in Figure 5. The initial value of N_i for the FU compartment (compartment 1) is equal to one when time equals zero, or N(0)=0. All other compartments in the model are zero at t=0.

- λ_{ji} is the first order rate constant ($time^{-1}$) from compartment j to compartment i. The first term in the right side of Equation 4 represents the summation of all the jth compartments which flow into the ith compartment.

- λ_{ij} is the first order rate constant ($time^{-1}$) from compartment i to compartment j. The second term in the right side of Equation 4 represents the summation of all the ith compartments that flow into the jth compartment.

The amount of FU or metabolite in each compartment at any time after the onset of exposure is determined by solving a differential equation that follows the form shown in Equation 4. Each compartment has a separate differential equation. Using the Stella modeling program, the amount of FU or metabolite in each compartment is calculated for a time period of 12 hours (to simulate the time period over which data were collected in experiments). The model is solved by a time step numerical solution using the Runge-Kutta 4 numerical method of solving differential equations (Gerald, 1970). The time step was chosen to be 1/10th the smallest half-life in each model to ensure accuracy of the numerical solution. In addition, a test of the validity of this time-step size was conducted by sequentially reducing the time-step and comparing the predicted concentrations of FdUMP at 3 hours. Changing the time-step to values smaller than $1/10^{th}$ the smallest half-life produced

less than a 1% change in the predicted FdUMP concentrations. Each of the four stages in rat biological development used a different time step since the half-lives for transformation differed.

The following system of differential equations was used to calculate the amount of FU or each metabolite (the right-most column shows the compound modeled by the corresponding differential equation):

(5)	$dN_1(t)/dt = \lambda_{21}N_2(t) - \lambda_{13}N_1(t) - \lambda_{12}N_1(t) - \lambda_{cat}N_1(t)$	FU
(6)	$dN_2(t)/dt = \lambda_{12}N_1(t) - \lambda_{23}N_2(t) - \lambda_{21}N_2(t)$	FUrd
(7)	$dN_3(t)/dt = \lambda_{13}N_1(t) + \lambda_{23}N_2(t) - \lambda_{34}N_3(t)$	FUMP
(8)	$dN_4(t)/dt = \lambda_{34}N_3(t) - \lambda_{45}N_2(t) - \lambda_{49}N_9(t)$	FUDP
(9)	$dN_5(t)/dt = \lambda_{45}N_4(t)$	FUTP
(10)	$dN_8(t)/dt = \lambda_{98}N_9(t)$	FdUMP
(11)	$dN_9(t)/dt = \lambda_{49}N_4(t) - \lambda_{910}N_{10}(t) - \lambda_{98}N_9(t)$	FdUDP
(12)	$dN_{10}(t)/dt = \lambda_{910}N_9(t)$	FdUTP

The time-step numerical solutions to these equations were generated using the STELLA simulation software, as shown in Table 1.

Table 1. Stella Time Step Numerical Equations. This table shows the time-step equations used in Stella to simulate the differential equations underlying the system of FU transformation.

FdUDP(t) = FdUDP(t – dt) + (RR – P4 – P3) * dt

```
INIT FdUDP = 0
RR = FUDP*L49
P4 = FdUDP*L98
P3 = FdUDP*L910

FdUMP(t) = FdUMP(t - dt) + (P4) * dt

INIT FdUMP = 0
P4 = FdUDP*L98

FdUTP(t) = FdUTP(t - dt) + (P3) * dt

INIT FdUTP = 0
P3 = FdUDP*L910

FU(t) = FU(t - dt) + (UP21 - UP12 - OPRT13 - DPD) * dt

INIT FU = 1
UP21 = Furd*L21
UP12 = FU*L12
OPRT13 = FU*L13
DPD = FU*Lcat

FUDP(t) = FUDP(t - dt) + (P1 - P2 - RR) * dt

INIT FUDP = 0
P1 = FUMP*L34
P2 = FUDP*L45
RR = FUDP*L49

FUMP(t) = FUMP(t - dt) + (UK23 + OPRT13 - P1) * dt

INIT FUMP = 0
UK23 = Furd*L23
OPRT13 = FU*L13
P1 = FUMP*L34

Furd(t) = Furd(t - dt) + (UP12 - UK23 - UP21) * dt

INIT Furd = 0
UP12 = FU*L12
UK23 = Furd*L23
UP21 = Furd*L21

FUTP(t) = FUTP(t - dt) + (P2) * dt

INIT FUTP = 0
P2 = FUDP*L45
```

Chapter 3. Model Parameters

3.1 Parameters for OPRTase, uridine phosphorylase, and uridine kinase

In creating this biologically-based metabolism model, the most difficult task was finding the reaction rates for each step in the metabolism of fluorouracil. The one study that separated the pathways into the initial steps leading to FdUMP was performed by Dr. Pauline Schwartz and other researchers at Yale University's School of Medicine. Enzyme activities were measured for OPRTase, uridine phosphorylase, and uridine kinase. This study included measurement of the metabolism in the backward direction with uridine phosphorylase; i.e. FUrd → FU (Schwartz et al. 1985).

The data in this paper were enzyme activities in the bone marrow and RPMI colon tumors of the rat. While it is known that most of the metabolism of FU occurs in the liver, this was the only data set available on the enzyme activities in the anabolism direction. The activities of bone marrow compared to colon tumor indicated that the tumor activity was 1.6 times that in bone marrow for the uridine phosphorylase reaction going from FU to FUrd (1 → 2). The tumor activity was 1.8 times that of the bone marrow in the UP reaction going from FUrd to FU (2→1); therefore, all other things being equal, the tumor rate constant should be higher than that in the bone marrow by a factor of 1.8 (since the rate constant is Vmax/Km). Schwartz et al. (1985) calculated Km values for both UP 1→2 and UP 2→1 in the rat liver and the RPMI colon tumor. When compared, the tumor Km was 1.6 times the Km of the liver in the 1→2 direction and 1.1 times the Km of the liver in the 2→1 direction; therefore, all other things being equal, the tumor rate constant should be less than the bone marrow rate constant by a factor of 1.1 to 1.6. Given the above calculations, the bone marrow rate constant would approximate the liver rate constant within a factor of 3 (it might be as much as a factor of 1.8 x 1.6 or 2.9 lower than that in the liver). This is not a large difference when dealing with biological data. Therefore, for lack of better data, it was assumed that the bone marrow activity could act as a surrogate for liver activity.

The enzyme activities measured, presented in moles product/mg protein/hr, were converted to a first-order rate constant. This was done in the following calculation:

$$(13) \quad \lambda = \frac{\text{Reaction Velocity } \left(\frac{\text{moles product}}{\text{mg protein} - \text{hr}}\right) \times \text{Protein (mg/ml)}}{\text{Reactant Concentration (moles/ml)}}$$

For example, in calculating λ_{13}:

$$\lambda_{13} = \frac{\left(\frac{15 \times 10^{-9} \text{ moles FUMP}}{\text{mg protein} - \text{hour}}\right)\left(\frac{2.75 \text{ mg protein}}{\text{ml}}\right)}{\frac{200 \times 10^{-9} \text{ moles FU}}{\text{ml}}}$$

or $\lambda_{13} = 0.21$ / hr

All rate constants based on the Schwartz et al. (1985) data were calculated in the same manner and can be seen in Table 2. The amount of protein used in the experiment was given as 2.75 mg protein/ml. The tissues were exposed initially to 200 μM FU, and measurements were done after one hour (by which time it is assumed that the FU concentration would be below 100μM and, therefore, first-order kinetics apply).

Table 2. Enzyme activity levels and lambda values for enzymes OPRTase, uridine phosphorylase, and uridine kinase from the Schwartz et al. data in the rat (1985).

	OPRTase	UP 1->2	UP 2->1	UK	
	λ_{13}	λ_{12}	λ_{21}	λ_{23}	
Enzyme activity	15	143	130	55	(nmoles/mg-p/hr)
Lambda values	0.21	1.97	1.79	0.76	(per hour)

3.2 Nucleoside diphosphate kinase

Kimura et al. (1985) researched the different aspects of nucleoside diphosphate kinase, or NDPK. Through this and numerous other studies mentioned in Kimura et al. (1985), it was decided that this enzyme is tightly associated with cell membranes and to a smaller extent in the cytosol. NDPK is responsible for the 'ping-pong' reaction sequences related to adding or removing a phosphate group from a nucleotide. The ping-pong mechanism has been described as a sequence of events in catalysis where one substrate is bound, one product is released, a second substrate comes in, and a second product is released (Mathews, 1990). However, the enzyme catalyzes this reaction in any ribo- or deoxyribonucleoside with a purine or pyrimidine base structure (Kimura et al. 1988). Therefore, it was decided that the activity for adding a phosphate group to GDP (GDP → GTP) would be a suitable surrogate for NDPK activity in the metabolism model for fluorouracil until better data are available.

Plasma membrane from rat liver cells were treated with 100μM of guanine diphosphate. The membrane-associated nucleoside diphosphate kinase activity was measured at 44±1 nmol/min/mg protein, or 2646 nmol/hr/mg protein. The enzyme assay was performed with a protein concentration of 2μg protein per 100μl tube. The lambda value was calculated as explained in the previous section and was found to equal 0.53 per hour (Table 3).

Table 3. Enzyme activities and lambda values of NDPK, RR, and DPD measured in the rat liver.

	NDPK	RR	DPD	
	λ_P	λ_{49}	λ_{cat}	
enzyme activity	2646	0.0006	24	(nmoles/mg-p/hr)
Lambda values	0.529	0.036	4.8	(per hour)

3.3 Ribonucleotide reductase

A major step in the metabolism of FU to FdUMP is the ribonucleotide reductase (RR) mediated reduction of FUDP to FdUDP. RR is a very complex enzyme which requires activation by adenosine triphosphate (ATP). Reduction of the pyrimidine ribonucleoside

diphosphates requires 1 to 2 mM ATP for both cytidine diphosphate (CDP) and uridine diphosphate (UDP). For uracil, the standard amounts of substrate and activator are approximately 0.05 μmole of UDP and 0.25 μmole of ATP (Moore et al. 1966).

The rat liver RR was studied by Elford et al. at the Medical College of Virginia (1977). The RR activity was measured during the conversion of CDP to dCDP. Although CDP, UDP, and FUDP are different compounds, it was decided in the present research that the activity for one nucleotide would be close enough to another nucleotide to be used in this model. It is also important to note that both CDP and UDP require the activation of ATP for the reduction reaction to take place (Moore et al. 1966).

In the absence of better data the RR from the CDP → dCDP reduction was used to estimate the FUDP → FdUDP reduction. The activity of RR in the liver of the control animals could not be detected. Therefore, an upperbound of the RR rate was calculated to be less than 0.6 μμmole/hr/mg protein, or 0.6×10^{-12} mole/hr/mg protein (Elford et al. 1977) and used to calculate the lambda value. The liver was treated with 0.12μM of radiolabeled CDP in a solution with 7.25 mg protein per ml. The lambda value (λ_{49}) was calculated as explained in the earlier sections and was found to be no more than 0.036 per hour (Table 3).

3.4 Dihydropyrimidine dehydrogenase

The enzyme DPD (dihydropyrimidine dehydrogenase) is responsible for the clearance of FU and this initial step of catabolism competes with the anabolism pathway. Naguib et al. (1985) measured the DPD activity in the rat liver when exposed to fluorouracil. The liver tissue cells were exposed to a 25 μM dose of FU during incubation. The solution was found to have a concentration of 400±3 pmol/min/mg protein, or 24 nmol/hr/mg protein. These data were used to calculate the lambda value for the DPD enzyme activity as shown in the earlier section. The lambda value for DPD (λ_{cat}) was found to be 4.8/hr (Table 3).

3.5 Uridine Kinase activity changes during development

Enzyme amounts change during the development process. All of the above enzyme activities were measured in an adult rat or adult rat tissue. To incorporate the changes during development, the enzymes must be scaled to the different points in development. Unfortunately, the enzyme data for developing rats could not be found for each of the

enzymes involved in the process. Actually, only one enzyme could be found with detailed data from numerous different points in development. This one enzyme was uridine kinase (UK). The Herzfeld et al. study looked at the changes in UK activity in a rodent as measured at gestation day (gd) 20 or 21, and postnatal days 9, 12, and 60-90 (adult). The physiological significance of the changing activity of this enzyme during development is not fully understood (Herzfeld et al. 1979). The data on UK activity were used to create a ratio of change at the different points of development versus the adult activity level (Table 4).

Table 4. The UK activity with uracil (nmol/min/g tissue) over development and the ratio compared to the adult activity in the rat liver using data from the Herzfeld et al. study (1979).

age	UK activity	age/adult
Fetal (gd 20-21)	75.5	2.86
9 days old	49.1	1.86
12 days old	56.6	2.14
60-90 (adult)	26.4	1

The ratios were used to scale most of the enzyme activity lambda values to allow the creation of a model for each of the four points of development measured by Herzfeld et al. (1979). The DPD enzyme was the only value not scaled to the UK ratios. A study by Tateishi et al. (1997) measured the amount of DHFU and FUPA produced in the reaction with DPD and found no significant alteration among various age rats of both sexes. They concluded that no gender-differences or age-differences exist in the hepatic activity of DPD. This study looked primarily at rats from 3 weeks to >60 weeks old. It could be possible to find differences if the activities were measured in younger rats, but until these data are available for fluorouracil it was decided to keep the DPD activity constant for the four development points in this FU metabolism model. The final lambda values used in the current metabolic model are listed in Table 5.

Table 5. Enzyme activity lambda values after adjustment for the age of the rat.

Enzyme activity Lambda values
(per hour)

age	OPRT Lambda 1-3	UP Lambda 1-2	UP Lambda 2-1	UK Lambda 2-3	RR Lambda 4-9	NDPK Lambda P	DPD Lambda out
fetal	0.60	5.63	5.12	2.17	0.10	1.52	4.8
day 9	0.39	3.66	3.33	1.41	0.07	0.99	4.8
day 12	0.45	4.22	3.84	1.63	0.08	1.14	4.8
adult	0.21	1.97	1.79	0.76	0.036	0.53	4.8

3.6 The Effect of Michaelis-Menten Kinetics

The rate constants reported in Tables 2-5 were obtained assuming first-order kinetics. While this approximation is valid for concentrations of FU below 100μM, at least one of the experiments (used to generate the results in Table 2) was conducted over a period of time during which the concentration is decreasing from the region where it is first-order. In this section, the issue of the degree of error potentially introduced by the assumption of first-order kinetics is addressed.

For two of the rate constants in Table 2 (the rate constants from 1 to 2 and the reverse reaction from 2 to 1), both Vmax and Km may be estimated from data on the reaction rates in tumors (note that Table 2 applies to bone marrow, so calculations below will not reproduce the numerical values in Table 2). For the reaction from 1 to 2, if it is assumed that the velocity measured in the experiment is Vmax (i.e. the reaction is at saturation), the value of Vmax is 230 nmol/mg protein/hr (Schwartz et al. 1985). The reported value of Km for the same experiment is 60 μM. With a protein concentration of 2.75 mg protein/ml (2750 mgP/L), the ratio of Vmax over Km is:

$$Vmax/Km = 2750\ (mgP/L) \times 230\ (nmol/mgP/hr) / 60000(nmol/L) = 10.5\ hr^{-1}$$

Similarly for the reaction from 2 to 1:

$$Vmax/Km = 2750\ (mgP/L) \times 228\ (nmol/mgP/hr) / 60000(nmol/L) = 9.7\ hr^{-1}$$

These values may be compared to the first order rate constants calculated assuming first order kinetics are in effect. Again using the tumor data, the rate constant from 1 to 2 under first order kinetics is:

Rate constant = 230 (nmol/mgP/hr) x 2.75 (mgP/L) / 200 (nmol/L) = 3.2 hr^{-1}

and for the rate constant from 2 to 1:

Rate constant = 228 (nmol/mgP/hr) x 2.75 (mgP/L) / 200 (nmol/L) = 3.1 hr^{-1}

Now, considering the ratio of the rate constants under these two approaches, for the reaction from 1 to 2 the ratio is 10.5/3.2 or 3.3, and the ratio for the reaction from 2 to 1 is 9.7/3.1 or 3.1. This indicates that the first-order reaction rate constants appearing in Table 2 may be too low by a factor of up to 3 if the experiments on which they were based have been assumed incorrectly to have been conducted in the region where first order kinetics apply. This potential effect is considered further in the next chapter.

Chapter 4. Model Predictions and Sensitivity Analysis

4.1 Model Results

A separate model of FU metabolism was established for each of the four developmental points using the general structure shown in Figure 2 and the parameter values shown in Table 5. The adult model is the most reliable since the data used in establishing rate constants are directly from adult laboratory rats. The other three models are conditional upon the assumption that all enzymes are affected by development in the same age-dependent manner as uridine kinase. The liver was modeled because the metabolism data was available in the rat liver. The results of the model runs and the sensitivity analysis are described in the following sections.

4.2 Results in the adult rat model

It would be ideal to test this model against FdUMP measurements from laboratory data. Unfortunately, no study was found that measured the amount of FdUMP produced after a bolus dose of FU in a rat. A study was found (Arellano et al. 1997) which recorded the amount of FUDP produced in an isolated rat liver (which removes the need to model translocation) after administration of FU. Since FUDP becomes FdUDP through ribonucleotide reductase, followed by dephosphorylation of FdUDP to FdUMP, using these data is still a relatively good way to check the model's ability to predict FdUMP.

The measured amount of FUDP at 3 hours after FU administration in the Arellano et al. study (1997) was 0.16% of the administered FU dose. The adult rat model developed in the present study (with the initial value of 1 in the FU compartment and 0 in all other compartments, and with λ values as shown in Table 5) estimated that FUDP is 0.048 at three hours after administration of an initial quantity of 1 unit of FU (Figure 6). Therefore, 4.8% of the original dose was predicted to become FUDP at 3 hours after exposure in the model. When comparing the two results, the model presented in this paper estimated 30 fold more FUDP (0.048/0.0016) than was actually measured in the Arellano et al. study (1997). As for

FdUMP, the adult model predicted that 0.1% of the dose of FU would become FdUMP 3 hours after the exposure (see Figure 7).

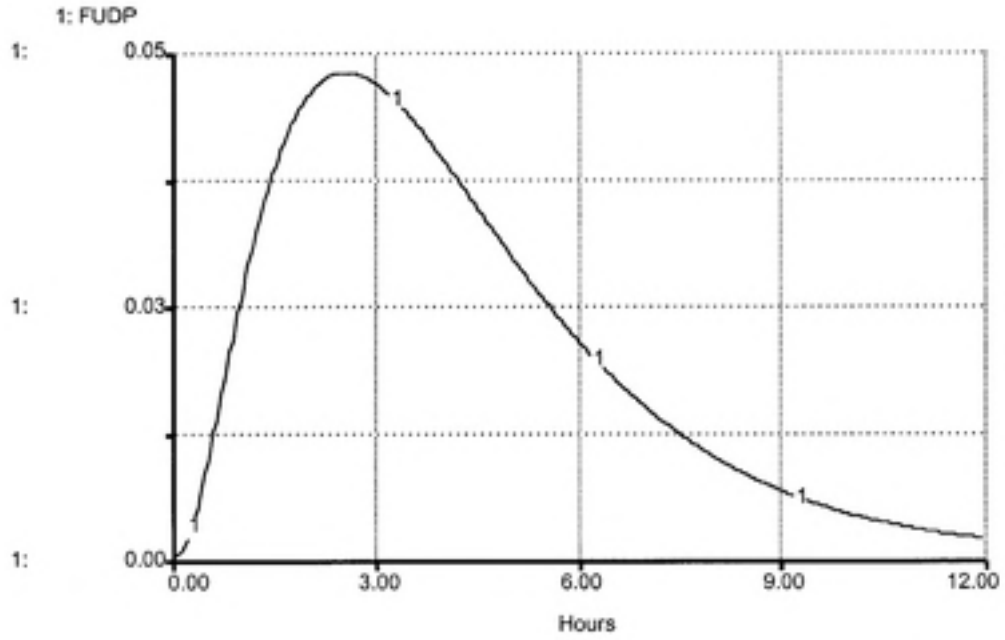

Figure 6. The predicted amount of FUDP formed by metabolism using the adult rat model as a function of time. The administered dose of FU is 1 unit and the initial amount in all other compartments (i.e. initial amount of all metabolites) is 0. Note the value at t equal 3 hours is approximately 0.048. The X represents the value measured at 3 hours by Arellano et al. (1997) which is approximately 0.0016±0.0004.

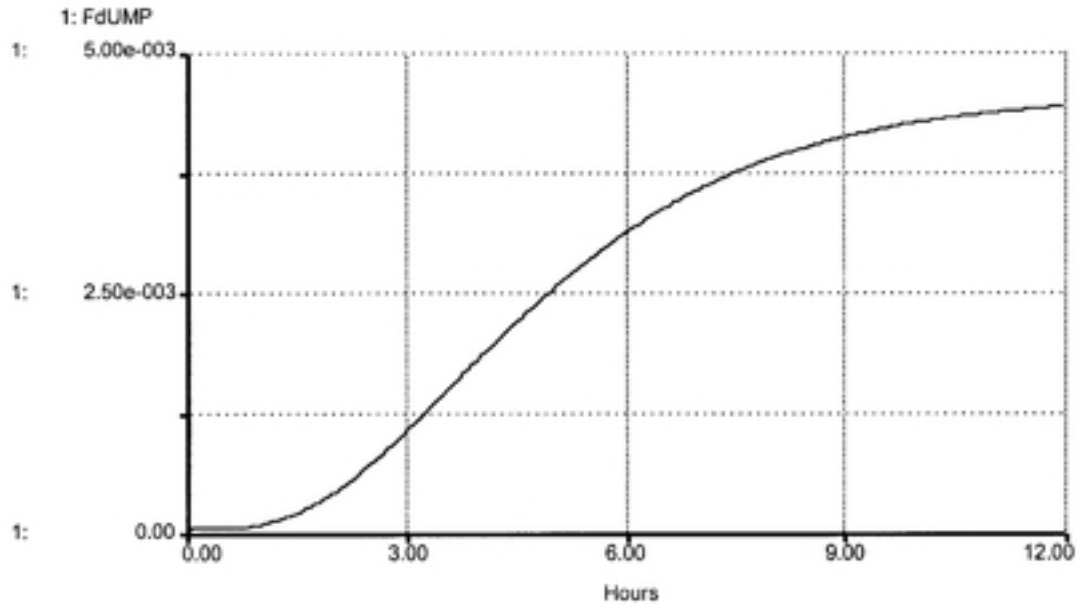

Figure 7. The predicted amount of FdUMP formed by metabolism using the adult rat model over time, with an administered dose of FU of 1 unit.

4.3 Results in the 12 day old rat model

Using the parameters for the 12 day model given previously in this paper, the FUDP and the FdUMP were estimated for the 12 day old rat. Results are shown in Figures 8 and 9 using the same initial conditions as in the adult model and the age-specific values for λ shown in Table 5. Approximately 3.3% of the original dose was transformed to FUDP at 3 hours after bolus administration of FU. In the same model, about 0.6% of the original dose of FU was converted to FdUMP by 3 hours.

4.4 Results in the 9 day old rat model

Using the parameters for the 9 day model given previously in this paper, the FUDP and the FdUMP were estimated for a 9 day old rat. Results are shown in Figures 10 and 11 using the same initial conditions as in the adult model and the age-specific values for λ shown in Table 5. Approximately 5.0% of the original dose was transformed to FUDP at 3 hours after bolus administration of FU. This was the highest level of FUDP of the four models. About 0.6% of the original dose was FdUMP. This is the same percent of the original dose that becomes FdUMP as was predicted in the 12 day model.

4.5 Results in the fetal rat model

Using the estimated fetal parameters, FUDP and FdUMP were calculated as a percent of the original dose using the fetal rat model. Results are shown in Figures 12 and 13 using the same initial conditions as in the adult model and the age-specific values for λ shown in Table 5. FUDP made up 2.5% of the original dose 3 hours after bolus administration of FU. This is the lowest value for FUDP of the four developmental stages calculated. As would be expected, the fetal calculation for FdUMP was the highest of the four stages. FdUMP was measured as 0.8% of the original dose at 3 hours after bolus administration of FU.

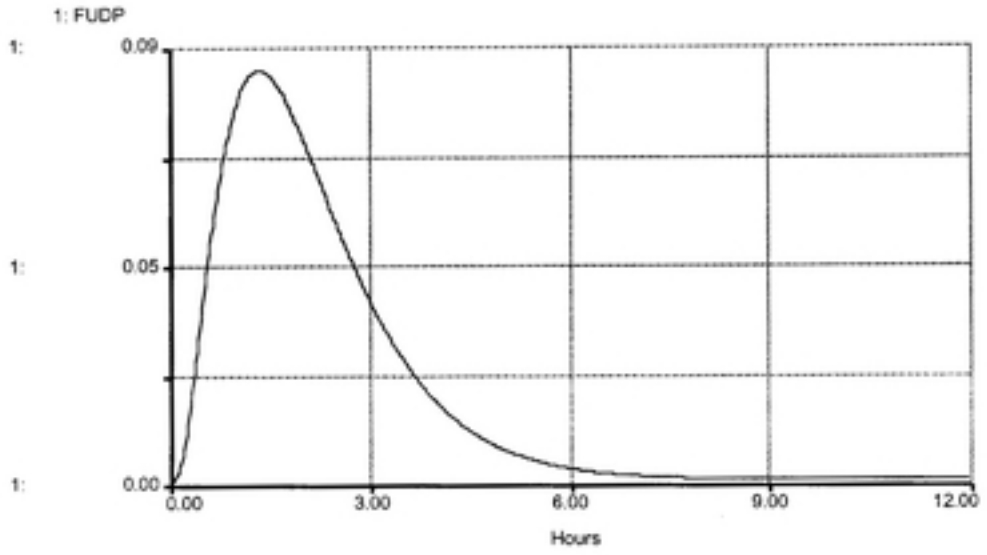

Figure 8. The predicted amount of FUDP formed by metabolism, using the 12 day old rat model, as a function of time, with an administered dose of FU = 1 unit.

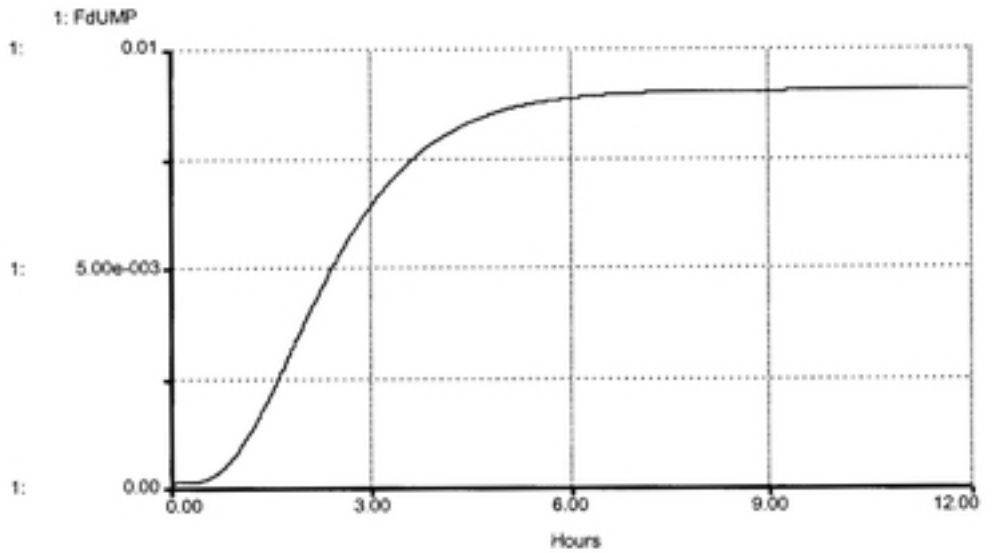

Figure 9. The predicted amount of FdUMP formed by metabolism, using the 12 day old rat model, as a function of time, with an administered dose of FU = 1 unit.

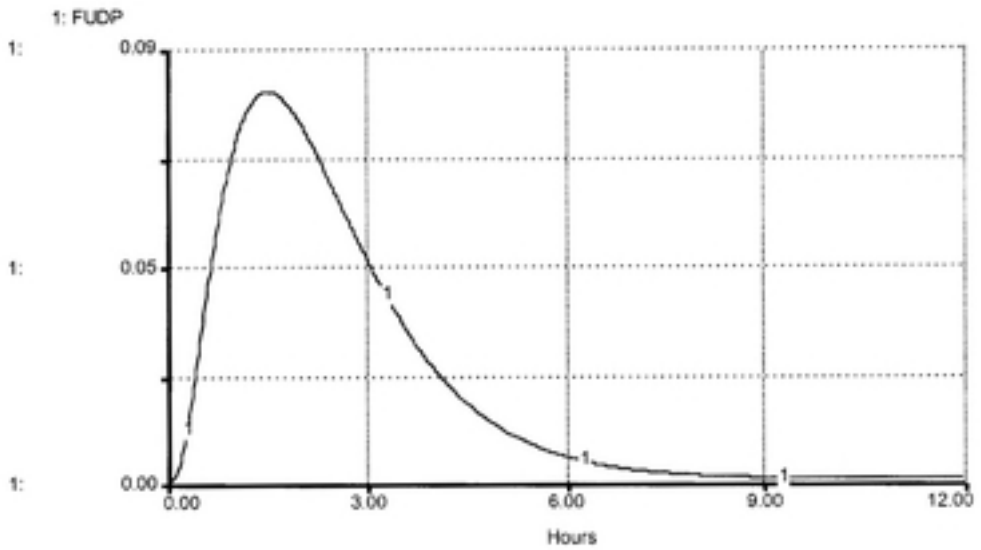

Figure 10. The predicted amount of FUDP formed by metabolism, using the 9 day old rat model, as a function of time, with an administered dose of FU = 1 unit.

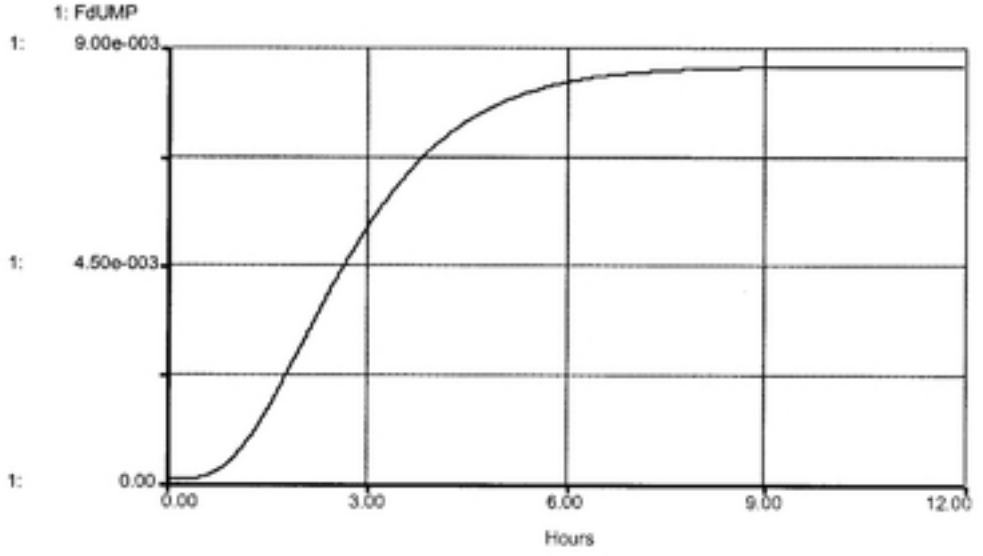

Figure 11. The predicted amount of FdUMP formed by metabolism, using the 9 day old rat model, as a function of time, with an administered dose of FU = 1 unit.

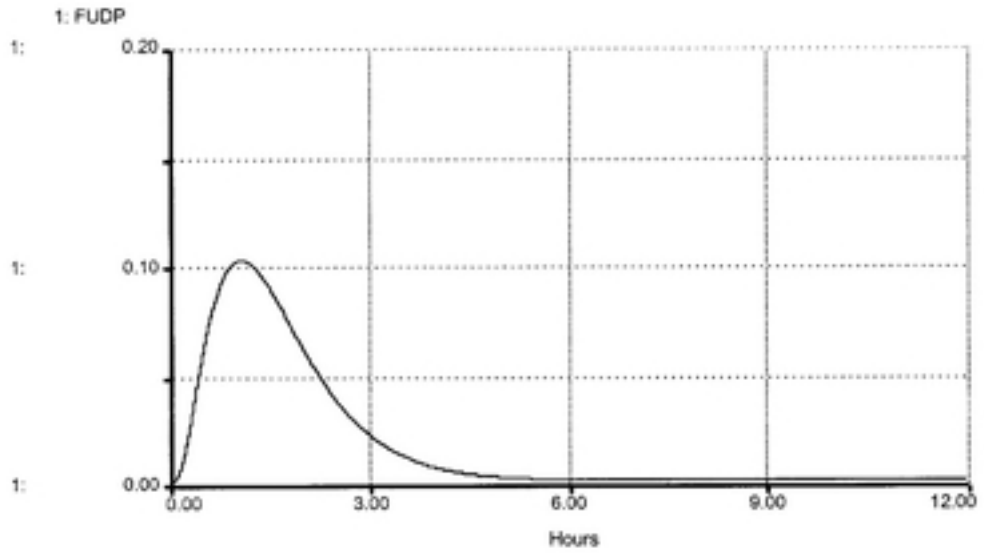

Figure 12. The predicted amount of FUDP formed by metabolism, using the fetal rat model, as a function of time, with an administered dose of FU = 1 unit.

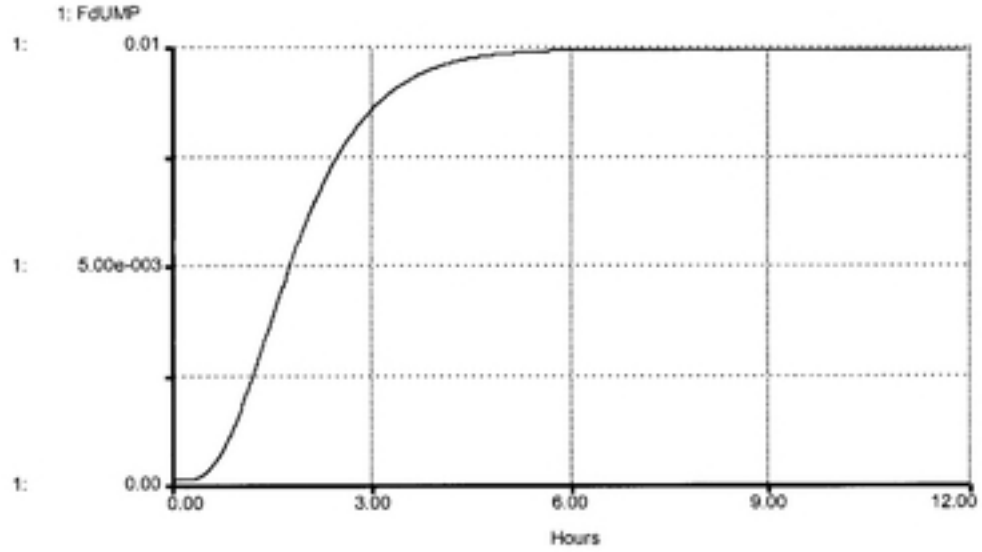

Figure 13. The predicted amount of FdUMP formed by metabolism, using the fetal rat model, as a function of time, with an administered dose of FU = 1 unit.

4.6 Uncertainty and Model Adjustments

The primary test of the model is the ability to fit data on the measured amount of FdUMP in the liver following an injection of FU (since FdUMP is the dose metric for the biologically-based dose-response models). As was noted in Section 4.2, there is an approximate 30-fold overestimation of the measured amount of FUDP in the liver 3 hours after administration using the baseline model (i.e. the model where all parameters are fully constrained to the values found in experiments on surrogates of the individual rate constants). In this section, possible adjustments to the model, and their constraints due to the data used to determine the various rate constants, are considered.

There are four possibilities to account for the discrepancy between the baseline model predictions and the data:

- The data were collected incorrectly, or do not reflect the conditions assumed by the model. This possibility is not considered further here, since the data are judged to be relevant to the modeled circumstances.
- The model is formulated incorrectly. Pathways of metabolism are missing and/or pathways have been included inappropriately. This possibility is not considered further here, since the model already incorporates the author's best judgements on each of these issues.
- The model is formulated correctly, but the kinetics of some of the reactions are not approximated adequately by first order kinetics (requiring Michaelis-Menton kinetics). This possibility is explored below.
- The model is formulated correctly, and the kinetics are described adequately by first order reactions, but the parameter values shown in Table 5 are incorrect. This possibility is explored below.

With respect to model parameters, it should first be noted that the rate constants for the transformations between 1 and 2, 1 and 3, 2 and 1, and 2 and 3 all are obtained from studies in which the 68% confidence interval on the measured reaction velocity are within 30% of the value used in calculating the rate constants in Table 5. This implies that these lambda values are not adjustable by more than approximately 60% (the 95% confidence

interval) without placing them outside the confidence intervals for the individual measurements. As a first step, these 4 rate constants were each adjusted by up to 60% to provide a better fit of the model to the 3 hour data point. In particular, the rate constant from 2 to 1 was increased and the other 3 rate constants were decreased. With these changes, the predicted curve of FUDP as a function of time is as shown in Figure 14. Next, the same 4 rate constants were adjusted by up to 30% to look at the 68% confidence interval. With this change made in the model, the predicted curve of FUDP as a function of time is shown in Figure 15.

Consider next the relative fraction of FU going towards the catabolic pathways rather than anabolic pathways. Given the parameter values in Table 5, the fraction predicted by the model is approximately 0.7. The existing data, however, suggest this fraction is between 0.7 and 0.95. If instead of using the study by Naguib et al. (1985) to determine the rate constant for the catabolic pathways, one uses the assumption that the fraction going by catabolism should be 0.95 (rather than 0.7), the rate constant for catabolism of FU should be 40 hr^{-1}. With this change made in the model, the predicted curve of FUDP as a function of time is as shown in Figure 16.

Another possibility is that the rate constant for transformation from FUMP to FUDP has been overestimated, since it was assumed equal to the measured value of the rate constant for adding a single phosphate to a diphosphate (Rosksoski, 1996). While λ_{34} represents FUMP $\rightarrow$ FUDP, the data used to estimate the rate constants for NDPK were measured using the GDP $\rightarrow$ GTP (Kimura et al. 1985). The energy required to add a single phosphate to a monophosphate, however, should be higher, implying the rate constant for the transformation from FUMP to FUDP should be lower. The rate constant from FUMP to FUDP, therefore, was adjusted downwards systematically to find a value for FUDP at 3 hours that is in agreement with the measured value of 0.0016. It was necessary to reduce this rate constant from 0.53 hr^{-1} to 0.01 hr^{-1}. The resulting graph is shown in Figure 17.

An additional possibility is that the 4 rate constants for the transformations between 1 and 2, 1 and 3, 2 and 1, and 2 and 3, and the rate constant for adding a single phosphate to a diphosphate have been improperly estimated. The 4 rate constants were adjusted by up to 30% to provide a better fit of the model to the 3 hour data point. In particular, the rate constant from 2 to 1 was increased and the other 3 rate constants were decreased. The rate

constant from FUMP to FUDP was adjusted down by a factor of 10 (to account for the difference in energy requirement). With these changes made in the model, the predicted curve of FUDP as a function of time is as shown in Figure 18. The amount of FUDP predicted at 3 hours was predicted to be 0.005.

Next, the 4 rate constants were adjusted by up to 60% to provide a better fit of the model to the 3 hour data point. The rate constant from 2 to 1 was increased and the other 3 rate constants were decreased. The rate constant from FUMP to FUDP was adjusted down by a factor of 10. With these changes made in the model, the predicted curve of FUDP as a function of time is as shown in Figure 19. The amount of FUDP predicted at 3 hours was predicted to be 0.0023, which is within the 95% confidence limits of the measured value. This set of adjusted rate constants provides the best estimate of FUDP for this model.

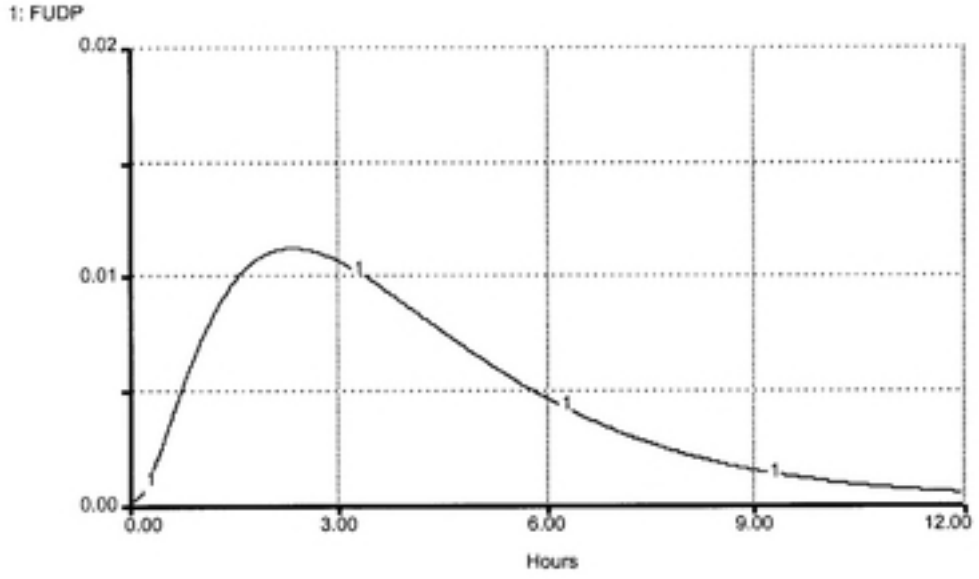

Figure 14. Predicted curve of FUDP after adjusting the rate constants by 60%. L12, L13, and L23 were decreased by 60%, while L21 was increased by 60%. Adjusting these four lambda values changed the 3 hour FUDP prediction from the original 0.048 to 0.012.

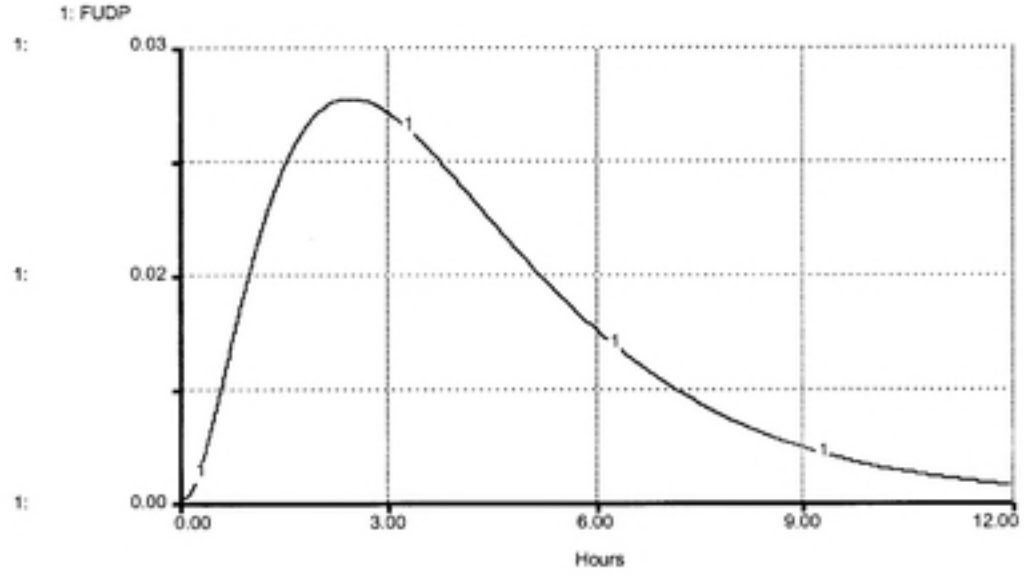

Figure 15. Predicted curve of FUDP after adjusting the 4 rate constants by 30%. L12, L13, and L23 were decreased by 30%, while L21 was increased by 30%. Adjusting these four lambda values changed the 3 hour FUDP prediction from the original 0.048 to 0.027.

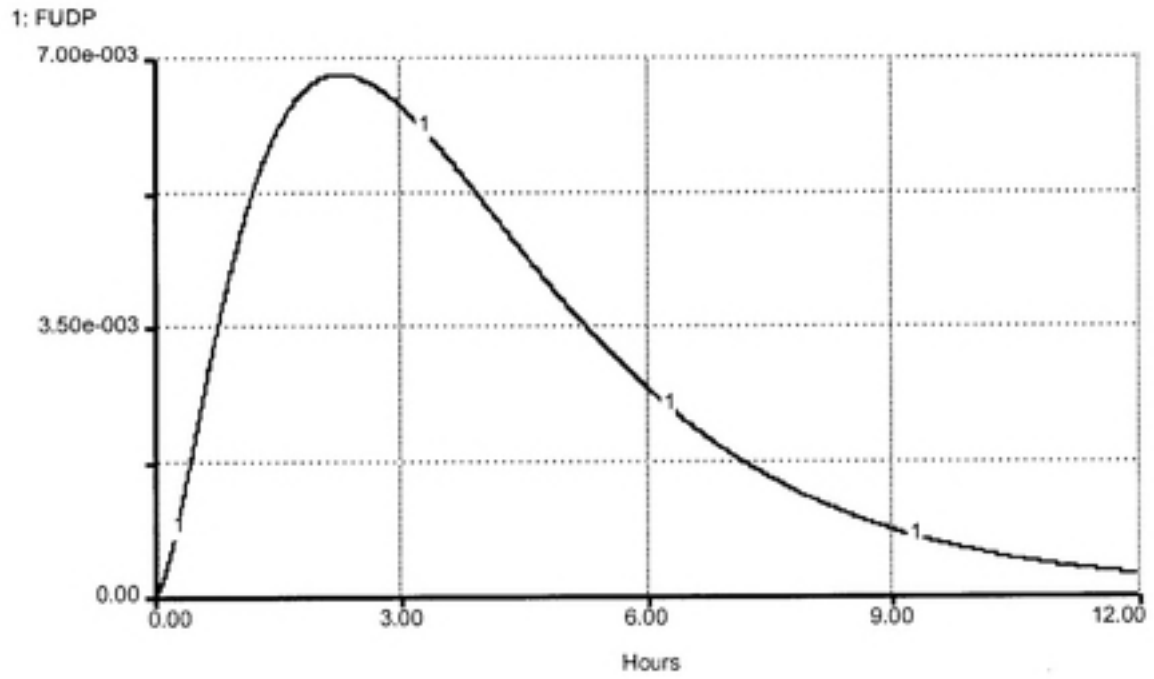

Figure 16. The predicted curve of FUDP after adjusting the Lcat so that 95% of FU is going the catabolism pathway. Adjusting this parameter changed the 3 hour FUDP prediction from the original 0.048 to 0.006.

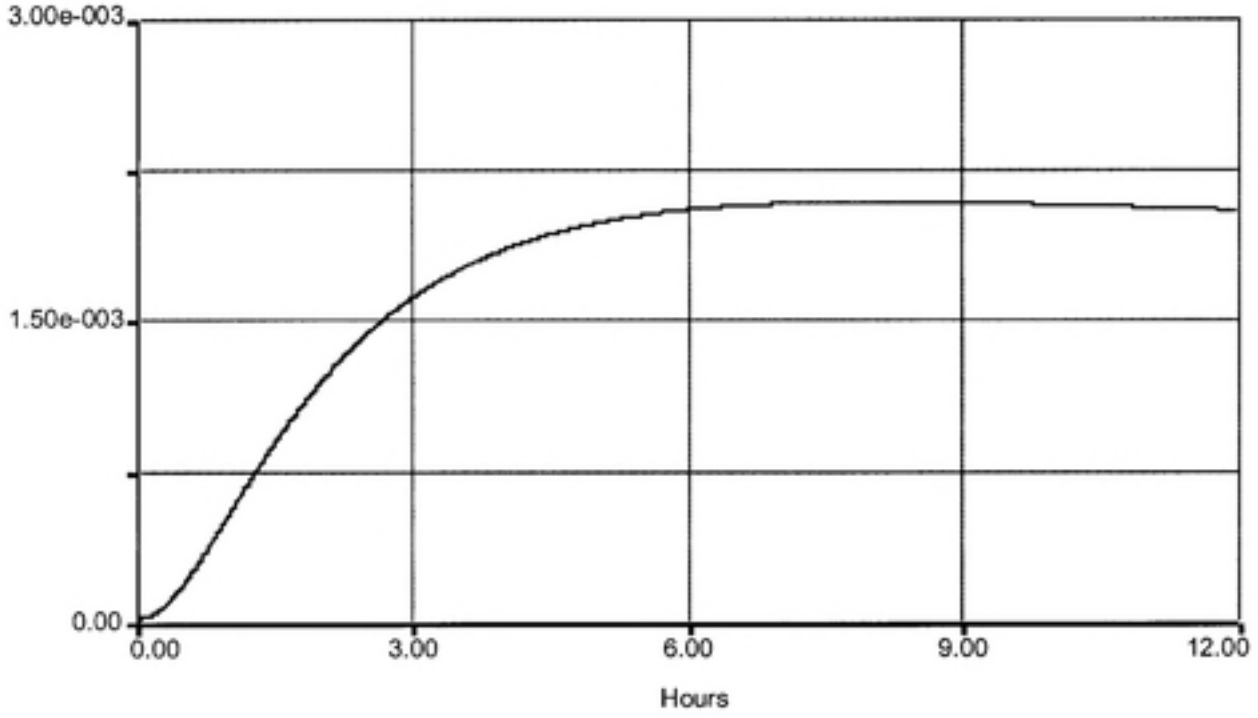

Figure 17. The resulting graph of FUDP after adjusting λ_{34} (FUMP to FUDP) downwards systematically to find a value for FUDP at 3 hours that is in agreement with the measured value of 0.0016. The value used for λ_{34} was 0.01 hr^{-1}.

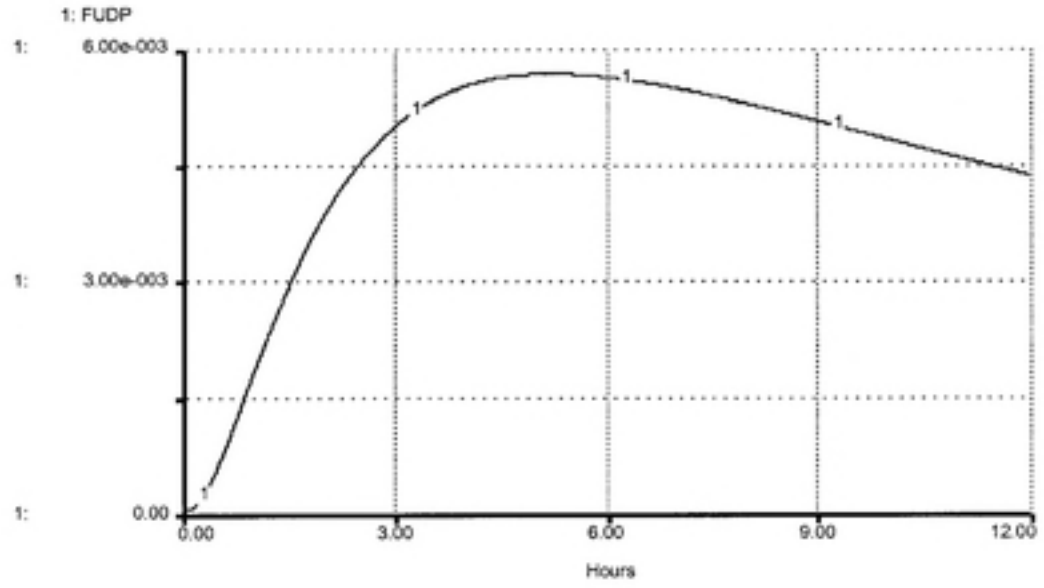

Figure 18. The resulting graph of FUDP after adjusting λ_{34} (FUMP to FUDP) downwards by a factor of 10 and adjusting L12, L13, and L23 down by 30%, and L21 up by 30%. The predicted amount of FUDP at 3 hours was 0.005.

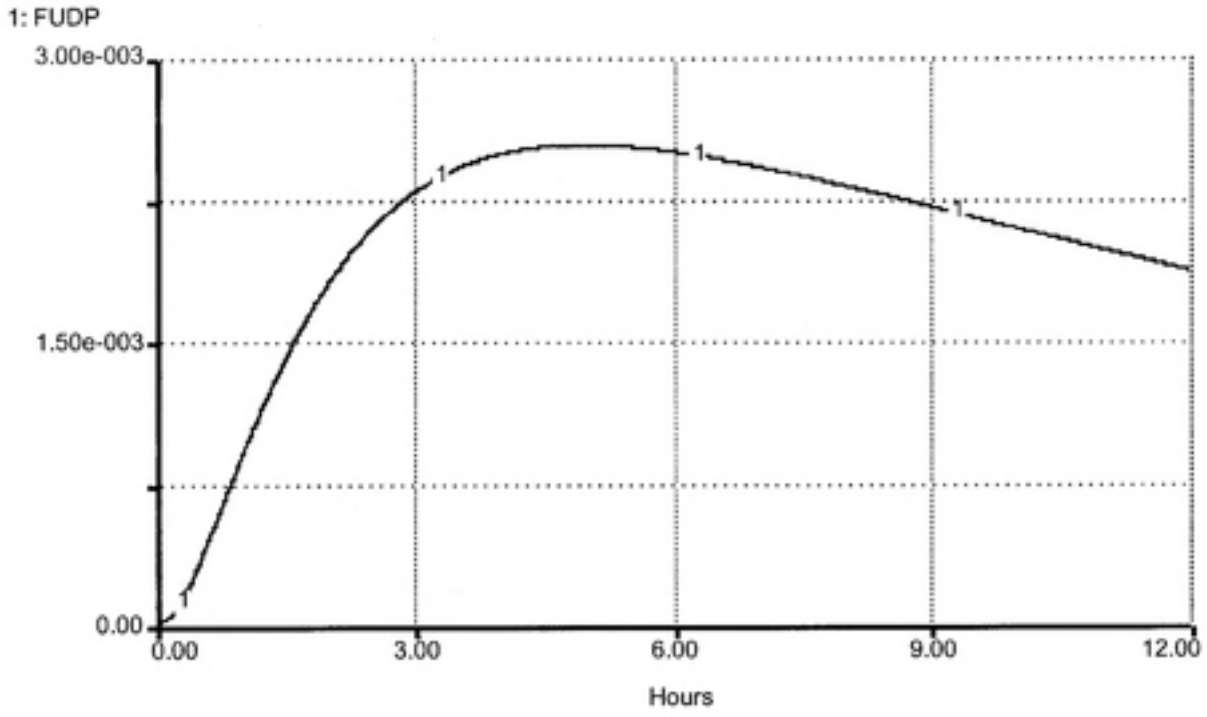

Figure 19. The resulting graph of FUDP after adjusting λ_{34} (FUMP to FUDP) downwards by a factor of 10 and adjusting L12, L13, and L23 down by 60%, and L21 up by 60%. The predicted amount of FUDP at 3 hours was 0.0023, which is within the 95% confidence of the measured value of 0.0016.

4.7 Sensitivity analysis

Each model was run with the original parameter value (from Table 5), constituting a baseline value, as well as a rate constant that is 50% above and 50% below the original parameter. This was done to each parameter with all other parameters remaining at the original values. The purpose of this exercise was to see if one parameter affected the overall model predictions more than the others, which would direct future research towards improving those parameters contributing most significantly to uncertainty in model predictions. Table 6 contains the values that were used for the sensitivity analysis for each of the model runs. Table 7 shows the changes seen in predicted FdUMP after 3 hours under each set of parameter values. The measure of sensitivity for a parameter was the absolute value of the difference in model predictions between the cases in which the parameter was increased by 50% and decreased by 50%. Changes in a specific λ value that produced a 1% change or greater in predicted FdUMP were assigned a +, while a - was assigned to changes of less than 1%. A minus sign does not mean that no change was measured for that specific lambda value, only that if one was measured it was less than 1%.

Table 6. Lambda values for sensitivity analysis (50% of original lambda value was subtracted (down) from or added (up) to the baseline lambda value from Table 5). (Lambda P represents L34, L45, L910, and L98)

	OPRT Lambda 1-3	UP Lambda 1-2	UP Lambda 2-1	UK Lambda 2-3	RR Lambda 4-9	NDPK Lambda P	DPD Lambda out
fetal							
down	0.3003	2.8170	2.5596	1.0867	0.0515	0.7579	2.4000
up	0.9009	8.4509	7.6787	3.2602	0.1544	2.2736	7.2000
day 9							
down	0.1953	1.8320	1.6646	0.7067	0.0335	0.4929	2.4000
up	0.5859	5.4959	4.9937	2.1202	0.1004	1.4786	7.2000
day 12							
down	0.2251	2.1118	1.9188	0.8147	0.0386	0.5681	2.4000
up	0.6753	6.3353	5.7565	2.4441	0.1158	1.7044	7.2000
adult							
down	0.1050	0.9850	0.8950	0.3800	0.0180	0.2650	2.4000
up	0.3150	2.9550	2.6850	1.1400	0.0540	0.7950	7.2000

Table 7. The absolute value of the difference in the amount of FdUMP measured at 3 hours when using the lambda values from Table 6 in the models. The plus sign represent those which had a difference of 0.01 or greater, and the minus sign represents those which had a difference of less than 0.01. No measured difference was greater than 0.01.

age	L1-3	L1-2	L2-1	L2-3	L4-9	L3-4	L4-5	L9-10	L9-8	Lcat
fetal	--	--	--	--	+	--	--	--	--	--
day 9	+	+	+	+	+	+	+	+	+	+
day 12	--	+	--	+	+	+	+	--	+	+
adult	--	--	--	--	--	--	--	--	--	--

Using the results of the sensitivity analysis, it may be seen that each model (i.e. the models at different ages) was most sensitive to different parameters. However, this analysis indicates that the model is most consistently sensitive to the rate constant for ribonucleotide reductase (RR, Lambda 4-9). The enzyme that converts FUDP to FdUDP, where it is then available to become FdUMP, is the process which has the greatest impact on the amount of FdUMP produced. This sensitivity analysis suggests further investigation in almost all of the parameters, with a focus initially on the ribonucleotide reductase enzyme process followed in order by the UP, UK, NDPK, and DPD processes.

Chapter 5. Conclusions

5.1 Summary of metabolism model

The metabolism model presented in this paper was created to determine the amount of FdUMP that is formed when FU is introduced into the liver of a rat. The adult rat model estimated that 4.8% of the original dose became FUDP at 3 hours after exposure, while the available data indicate closer to 0.16%. Therefore, this baseline model (fully constrained by individual measured values for surrogates of the various rate constants) estimated 30 fold more FUDP than was actually measured (Arellano et al. 1997). Using the same model, it was estimated that 0.1% of the original dose of FU would have been metabolized to FdUMP 3 hours after the exposure. The model of the 12 day old rat and the 9 day old rat found that about 0.6% of the original dose became FdUMP. FdUMP was calculated at 0.8% of the original dose after 3 hours in the fetal rat model.

Even given the nature of modeling using biological data from numerous sources, a 30 fold overestimation is too large to be ignored. As a result, several plausible adjustments to model parameters were made to determine if a better fit could be obtained without exceeding the error bars on any single measurement of a surrogate rate constant. Several sets of adjustments were examined:

- The rate constants for the transformations between 1 and 2, 1 and 3, 2 and 1, and 2 and 3 were adjusted by 30% (within the 68% confidence interval error bars for the data on which these rate constants may be determined independently) and then by 60% (within the 95% confidence interval error bars). In particular, the rate constant for 2 to 1 was increased and the other 3 rate constants were decreased.
- The rate constant for the transformation between 3 and 4 was decreased based on the concept that the energy required to add a single phosphate to a monophosphate would be higher than adding a single phosphate to a diphosphate. This higher energy need should then imply that the rate constant is lower for the addition to the monophosphate.
- The rate constant for the catabolic pathway was increased to produce a prediction of 95% of the FU going by the catabolic pathways (and 5% by the anabolic pathways).

A combination of the first two changes above produced the best estimation of FUDP production. When adjusting the 4 rate constants mentioned in the first bullet by 60% and the rate constant for the transformation between 3 and 4 by a factor of ten, the amount of FUDP predicted by the model was within the 95% confidence limits of the measured value from Arellano et al. (1997). Since this combination of adjustments produces rate constants that are all consistent with the experimental data (at least within the 95% confidence bounds on those data, and within the assumption that adding a first phosphate requires significantly greater energy than adding subsequent phosphates), it seems reasonable to conclude that the model is capable of reasonable adjustment to fit the data on FUDP production.

There are many possible reasons for any residual differences between model predictions and measured values of FUDP. It is possible that the enzyme activity data was collected incorrectly from the laboratory studies. Pathways being added or left out of the model could be another source of error. The concern about what kinetics to use has been discussed as an area of concern. Calculations to determine the parameter values could also be questioned.

The model presented in this paper represented most, but not all of the known processes of FU metabolism. As mentioned earlier, the backflow was specifically measured in only one reaction. Assuming the amount of final product will take this into consideration does not provide the actual amount of metabolites that convert back to the parent compound. This model represents known processes as well as possible given the assumptions made and the data available.

The group which measured the 0.16% value (Arellano et al. 1997) performed the tests on an isolated rat liver, while most of the studies from which the parameters came used homogenized rat liver or rat liver cells. The limited access of the entire liver to the FU in the exposure solution could then produce a smaller amount of metabolites. As was mentioned earlier, the Kupffer cells of the liver have the highest level of UP activity. The Kupffer cells tend to adhere to the endothelial lining, therefore they would more accessible with liver homogenate or liver cells than in a whole liver (Liu et al. 1998).

It could be assumed from the results of the model presented in this paper that the fetal rat would have the most damage due to FdUMP complications, such as TS inhibition,

compared to the other three stages of development. This is supported by the sensitivity analysis which found the enzyme which converts FUDP to FdUDP, where it is then available to become FdUMP, as the process which has the greatest impact on the amount of FdUMP produced in most of the models. In general, a very small percentage of the FU dose actually becomes the metabolite FdUMP.

There are definite questions surrounding the model presented in this paper. Numerous assumptions were made dealing with the parameters. The major reason for the assumptions was the lack of better data. Each enzyme was represented by actual activity measurements, none were estimated. Therefore, the rates were based on measurements made using the liver of laboratory rats. The parameters that went into this model were calculated from the best information currently available.

This metabolism model was created to study the enzyme process in one species. The immediate goal of this model was to determine how much of the metabolite FdUMP was formed in the rat liver. The bigger purpose, as was explained in detail in the Introduction, is to look at the usefulness of modeling to study nucleotide synthesis inhibitors. As for the kinetics issue, the amount of metabolite formed is related to the concentration of FU because the model was done in first order. Although the use of first order kinetics is questionable, it can be justified somewhat by the dose-response data. The overall dose-response relationship of the amount of FU given to a test animal and the amount of TS inhibition seen is linear at low doses (Setzer, unpublished)

The major strength of this FU anabolism model is that it is the first of its kind. Although FU has been studied for many years, the focus tends to be on the catabolism. This is evident when looking at the existing models for FU. All models available dealt with the catabolism. This model is definitely a rough sketch of what is actually needed, but it is a first attempt. Now that a metabolism model has been created for FU focusing on the anabolism, it is more evident where further research is needed.

5.2 Data gaps and limitations

The major data gaps in the metabolism model presented in this paper can be found in the enzyme reaction rates. Specifically, ribonucleotide reductase activity needs to be measured with FU as the substrate, given the importance of this process shown by the

sensitivity analysis. More knowledge is needed to understand the phosphorylation rates and how they differ between monophosphates, diphosphates, and triphosphates. It would be beneficial to have a better picture of the path in which FU most commonly travels, as well as if thymidine phosphorylase and thymidine kinase play a significant role in the FdUMP production which occurs in the rat liver. Due to a lack of available information on the enzyme reaction rates, FU was not always the product used in the enzyme reactions performed in laboratory studies where the rates were measured. All of these things, if improved upon, would make a stronger and more accurate model.

The main limitation in understanding the metabolism of FU concerns the back-flow from metabolites to the parent compound. Most of the reactions in this metabolism model are reversible. Limited information was available in the literature on this subject.

5.3 Suggestions for future studies

An important issue that must be addressed before this model is improved upon is the use of first order kinetics. Most of the parameters used in this model were measured with low FU concentrations used in the reaction. However, as mentioned earlier, the Schwartz et al. data (1985) was not. When Dr. Pauline Schwartz was contacted, she believed that the activities provided in Schwartz et al. (1985) are close to the Vmax. With this information, it would not be unreasonable to think that the four parameters from this paper would then be an overestimation of what would be seen in a first order situation. It could not be determined if the assumption that the concentration would be under 100 μM at the time of the reaction measurements is correct. Therefore, it may be important to find a different source for these enzyme activities that used a lower concentration of FU. Another option is to change the entire model so that it follows M-M kinetics.

Another area of study could be to get data on each enzyme-driven reaction with 5-fluorouracil as the exposure material. Having this data in the rat at different stages of growth would increase our knowledge on how these processes change throughout development. Since the overall goal is to predict the amount of metabolites present in humans, it would be important to create a similar model with human data. The enzyme reaction rates with FU as the dose compound would have to be measured at different stages of human development. Due to the invasive nature of measuring the metabolites of FU (they are not present in the

blood, but only in the tissues) collecting these values would be difficult. Therefore, the next best thing would be to have a comparison of the enzyme concentrations at different stages of human development and the amount found in an experimental animal.

The goal of this research was to create a mathematical model of the metabolism of FU in the rat to link to the physiologically-based pharmacokinetic model being developed by the EPA (Setzer, unpublished). A biologically-based metabolism model was created with FU as the input and FdUMP is the major endpoint. Although this model is only of the rat liver, it is the first model for FU anabolism. The knowledge gained about FU as the test compound could help to determine if models are able to show the action of other compounds that interfere with nucleotide synthesis. Once such chemicals are better understood, models would be beneficial in making regulatory decisions.

REFERENCES

Absil J, Tuilie M, Roux JM. Electrophoretically distinct forms of uridine kinase in the rat. Tissue distribution and age-dependence. Biochemical Journal, 185(1): 273-276, 1980.

Akiba T, Okeda R, Tajima T. Metabolites of 5-fluorouracil, α-fluoro-β-alanine and fluoroacetic acid, directly injure myelinated fibers in tissue culture. Acta Neuropathol, 92: 8-13, 1996.

Anand AJ. Fluorouracil Cadiotoxicity. The Annals of Pharmacotherapy, 28: 374-378, 1994.

Ardalan B, Luis R, Jaime M, Franceschi D. Biomodulation of fluorouracil in colorectal cancer. Cancer Investigation, 16(4): 237-251, 1998.

Arellano M, Malet-Martino M, Martino R, Spector T. 5-Ethynyluracil (GW776): Effects on the Formation of the Toxic Catabolites of 5-FU, Fluoroacetate and Fluorohydroxypropionic acid in the Isolated Perfused Rat Liver Model. British J. Cancer, 76(9): 1170-1180, 1997.

Barberi-Heyob M, Weber B, Merlin JL, Dittrich C, de Bruijn EA, Luporsi E, Guillemin F. Evaluation of Plasma 5-FU Nucleoside Levels in Patients with Metastatic Breast Cancer: Relationships with Toxicities. Cancer Chemother. Pharmacol., 37: 110-116, 1995.

Beckman DA, Brent RL, Lloyd JB. Sources of amino acids for protein synthesis during early organogenesis in the rat. 4. Mechanisms before envelopment of the embryo by the yolk sac. Placenta, 17: 635-641, 1996.

Boike GM, Deppe G, Young JD, Malone JM, Malviya VK, Sokol RJ. Chemotherapy in a Pregnant Rat Model. Gynecologic Oncology, 34: 191-194, 1989.

Bose R, Yamada EW. Uridine phosphorylase activity of isolated plasma membranes of rat liver. Can. J. Biochem., 55: 528-533, 1977.

Cappiello M, Mascia L, Scolozzi C, Giorgelli F, Ipata PL. In vitro assessment of salvage pathways for pyrimidine bases in rat liver and brain. Biochimica et Biophysica Acta, 1425(2): 273-281, 1998.

Chaudhuri NK, Mukherjee KL, and Heidelberger, Charles. Studies on Fluorinated Pyrimidines. Biochemical Pharmacology, 1:328-341, 1985.

Cole RJ, Taylor NA, Cole J, Arlett CF. Transplacental effects of chemical mutagens detected by the micronucleus test. Nature, 227: 317-318, 1979.

Collins JM, Dedrick RL, King FG, Speyer JL, Myers CE. Nonlinear pharmacokinetic models for 5-fluorouracil in man: Intravenous and intraperitoneal routes. Clin. Pharmacol. Ther., 28(2): 235-246, 1980.

Diasio RB, Harris BE. Clinical Pharmacology of 5-Fluorouracil. Clinical Pharmacokinetics, 16: 215-237, 1989.

Dorko ME, Hayashi TT. Incorporation of labeled ribonucleic acid precursors into maternal and fetal rat tissues during pregnancy. Am. J. Obstet. Gynecol., 154: 801-805, 1986.

el Kouni MH, el Kouni MM, Naguib FNM. Differences in Activities and Substrate Specificity of Human and Murine Pyrimidine Nucleoside Phosphorylases: Implications for Chemotherapy with 5-Fluoropyrimidines. Cancer Research, 53: 3687-3693, 1993.

Elford HL, Bonner EL, Kerr BH, Hanna SD, Smulson M. Effect of Methotrexate and 5-Fluorodeoxyuridine on Ribonucleotide Reductase Activity in Mammalian Cells. Cancer Research, 37: 4389-4394, 1977.

Garnica AD, Chan W-Y. The role of the placenta in fetal nutrition and growth. J. American College of Nutrition, 15(3): 206-222, 1996.

Gerald CF. Applied Numerical Analysis. Reading, Massachusetts: Addison-Wesley Publishing Company, 1970.

Grafton TF, Bazare JJ, Hansen DK, Sheehan DM. The In Vitro Embryotoxicity of 5-Fluorouracil in Rat Embryos. Teratology, 36: 371-377, 1987.

Hamada A, Fukushima S, Saneyoshi M, Shimizu S, Kawaguchi T, Nakano M. Modulation of the Pharmacokinetics of 5-deoxy-5-fluorouridine and 5-FU in Rats by Oral Co-administration of Acyclothymidine. Biol. Pharm. Bull., 19: 729-732, 1996.

Harada M, Nishitani H, Koga K, Miura I, Umeno Y. Metabolism of Tegafur in Rat Liver Observed by *in vivo* ^{19}F Magnetic Resonance Spectroscopy and Chromatography. Jpn. J. Cancer Res., 83: 387-391, 1992.

Herzfeld A, Raper SM. Uridine Kinase Activities in Developing, Adult, and Neoplastic Rat Tissue. Biochem. J., 182: 771-778, 1979.

Hisata T. An Accurate Method for Estimating 5-Phosphoribosyl 1-Pyrophosphate in Animal Tissues with the Use of Acid Extraction. Analytical Biochemistry, 68: 448-457, 1975.

Horowitz R, Schwartz EL, Wadler S. Modulation of 5-FU by Interferon: a review of potential cellular targets. Medical Oncology, 12: 3-8, 1995.

Inaba M, Mitsuhashi J, Sawada H, Miike N, Naoe Y, Daimon A, Koizumi K, Tsujimoto H, Fukushima M. Reduced Activity of Anabolizing Enzymes in 5-FU-resistant Human Stomach Cancer Cells. Jpn. J. Cancer Res., 87: 212-220, 1996.

Ipata PL, Camici M. An Enzymatic Radioactive Assay to Determine Ribose-1-Phosphate in Tissue. Analytical Biochemistry, 112: 151-153, 1981.

Jackson RC. The role of ribonucleotide reductase in regulation of the deoxyribonucleoside triphosphate pool composition: Studies with a kinetic model. International Encyclopedia of Pharmacology and Theraputics, 128:127-150, 1989.

Joulia JM, Pinguet F, Grosse PY, Astre C, Bressolle F. Determination of 5-FU and its Main Metabolites in Plasma by High-performance Liquid Chromatography: Application to a Pharmacokinetic Study. J. Chromatography B, 692: 427-435, 1997.

Joulia JM, Pinguet F, Ychou M, Duffour J, Topart D, Grosse PY, Astre C, Bressolle F. Pharmacokinetics of 5-FU in Patients with Metastatic Colorectal Cancer Receiving 5-FU Bolus Plus Continuous Infusion with High Dose Folinic Acid (LV5FU2). Anticancer Research, 17: 2727-2730, 1997.

Juchau MR. Bioactivation in Chemical teratogenesis. Annu. Rev. Pharmacol. Toxicol., 29: 165-187, 1989.

Kao Y-H, Yang C-Y, Chen RRL, Huang J-D. Pulmonary Elimination of 5-Fluorouracil in Anesthetized Rats. J. Pharmaceutical Sciences, 74(10): 1095-1096, 1985.

Khor NP, Amyx H, Davis ST, Nelson D, Baccanari DP, Spector T. Dihydropyrimidine dehydrogenase Inactivation and 5-fluorouracil Pharmacokinetics: allometric scaling of animal data, pharmacokinetics and toxicodynamics of 5-fluorouracil in humans. Cancer Chemother. Pharmacol., 39: 233-238, 1997.

Kimura N, Shimada N. Differential Susceptibility to GTP formed from added GDP via membrane-associated nucleoside diphosphate kinase of GTP-sensitive adenylate cyclases achieved by hormone and cholera toxin. Biochem. Biophys. Res. Comm., 131(1): 199-206, 1985.

Kimura N, Shimada N. Membrane-associated Nucleoside Diphosphate Kinase from Rat Liver. J. Biol. Chem., 263(10): 4647-4653, 1988.

Kissel J, Brix G, Bellemann ME, Strauss LG, Dimitrakopoulou-Strauss A, Port R, Haberkorn U, Lorenz WJ. Pharmacokinetic analysis of 5-[^{18}F]fluorouracil tissue concentration measured with positron emission tomography in patients with liver metastases from colorectal adenocarcinoma. Cancer Research, 57(16): 3415-3423, 1997.

Koenig H, Patel A. Biochemical basis for fluorouracil neurotoxicity. Arch. Neurol., 23: 155-160, 1970.

Kuan H, Smith DE, Ensminger WD, Knol JA, DeRemer SJ, Yang Z, Stetson PL. Regional Pharmacokinetics of 5-FU in dogs, role of the liver, gastrointestinal tract, and lungs. Cancer Research, 58: 1688-1694, 1998.

LaCreta FP, Warren BS, Williams WM. Effects of pyrimidine nucleoside phosphorylase inhibitors on hepatic fluoropyrimidine elimination in the rat. Cancer Research, 49(10): 2567-2573, 1989.

Laskin JD, Evans RM, Slocum HK, Burke D, Hakala MT. Basis for Natural Variation in Sensitivity to 5-fluorouracil in Mouse and Human Cells in Culture. Cancer Research, 39: 383-390, 1979

Lau C, Mole ML, Copeland FM, Rogers JM, Kavlock RJ, Shuey DL, Cameron AM, Ellis D, Merriman J, Setzer RW. Toward building a biologically-based dose-response model for developmental toxicity of 5-fluorouracil in the rat: Acquisition of experimental data. Unpublished.

Liermann B, Matthes E, Langen P. Human tissues degrade uridine much less than thymidine. Possible consequence for 5-fluorouracil therapy. Biochemical Pharmacology, 33(5): 721-724, 1984.

Liu MP, Beigelman L, Levy E, Handschumacher RE, Pizzorno G. Discrete roles of hepatocytes and nonparenchymal cells in uridine catabolism as a component of its homeostasis. Am. J. Physiol. 274(37): G1018-G1023, 1998.

Lokich J. Improving 5-FU: biomodulation, pharmacomodulation, or infusional administration schedules? Cancer Investigation, 16(4): 293-294, 1998.

Luecke RH, Wosilait WD, Pearce BA, Young JF. A Physiologically Based Pharmacokinetic Computer Model for Human Pregnancy. Teratology, 49: 90-103, 1994.

Mader RM, Sieder AE, Braun J, Rizovski B, Kalipciyan M, Mueller MW, Jakesz R, Rainer H, Steger GG. Transcription and activity of 5-FU converting enzymes in fluoropyrimidine resistance in colon cancer in vitro. Biochemical Pharmacology, 54: 1233-1242, 1997.

Machara Y, Sakaguchi Y, Kusumoto T, Kusomoto H, Sugimachi K. Species Differences in Substrate Specificity of Pyrimidine Nucleoside Phosphorylase. J. Surgical Oncology, 42: 184-186, 1989.

Mathews CK, van Holde KE. Biochemistry. Redwood City, California: The Benjamin/Cummings Publishing Company, Inc., 1990.

McSheehy PMJ, Seymour MT, Ojugo ASE, Rodrigues LM, Leach MO, Judson IR, Griffiths JR. A Pharmacokinetic and Pharmacodynamic Study *in vivo* of human HT29 tumours using ^{19}F and ^{31}P magnetic resonance spectroscopy. European J. Cancer, 33(14): 2418-2427, 1997.

Mentre F, Steimer J-L, Sommadossi J-P, Diasio RB, Cano J-P. A Mathematical Model of the Kinetics of 5-Fluorouracil and its Catabolites in Freshly Isolated Rat Hepatocytes. Biochemical Pharmacology, 33(17): 2727-2732, 1984.

Moore EC, Hurlbert RB. Regulation of Mammalian Deoxyribonucleotide Biosynthesis by Nucleotides as Activators and Inhibitors. J. Biol. Chem., 241: 4802-4809, 1966.

Myers CE. The pharmacology of the fluoropyrimidines. Pharmacological Reviews, 33(1): 1-15, 1981.

Naguib FNM, Kouni MH, Cha S. Enzymes of uracil catabolism in normal and neoplastic human tissue. Cancer Research, 45: 5405-5412, 1985.

Naguib FNM, Soong S-J, el Kouni MH. Circadian Rhythm of Orotate Phosphoribosyltransferase, Pyrimidine Nucleoside Phosphorylases and Dihydrouracil Dehydrogenase in Mouse Liver. Biochemical Pharmacology, 45(3): 667-673, 1993.

Naser-Hijazi B, Berger MR, Schmahl D, Schlag P, Hull WE. Locoregional administration of 5-fluoro-2-deoxyuridine (FdUrd) in Novikoff hematoma in the rat: effects of dose and infusion time of tumor growth and on FdUrd metabolite levels in tumor tissue as determined by ^{19}F-NMR spectroscopy. J. Cancer Res. Clin. Oncol., 117: 295-304, 1991.

O'Flaherty EJ, Scott W, Schreiner C, Beliles RP. A physiologically based kinetic model of rat and mouse gestation: disposition of a weak acid. Toxicology and Applied Pharmacology, 112: 245-256, 1992.

Parker WB, Cheng YC. Metabolism and mechanism of action of 5-FU. Pharmac. Ther., 48: 381-395, 1990.

Peters GJ, Laurensse E, Leyva A, Lankelma J, Pinedo HM. Sensitivity of human, murine, and rat cells to 5-fluorouracil and 5'-deoxy-5-fluorouridine in relation to drug-metabolizing enzymes. Cancer Research, 46(1): 20-28, 1986.

Peters GJ, van Groeningen CJ, Pinedo HM. Dihydropyrimidine dehydrogenase in livers from mouse and rat, and in human liver, colon tumors, and mucosa in relation to anabolism of 5-fluorouracil. Purine and Pyrimidine Metabolism in Man IX, ??:633-636, 1998.

Pinedo HM, Peters GFJ. Fluorouracil: Biochemistry and Pharmacology. J. Clinical Oncology, 6(10): 1653-1664, 1988.

Raisonnier A, Bouma M-E, Salvat C, Infante R. Metabolism of Orotic Acid: Lack of Orotate Phosphoribosyltransferase in Rat Intestinal Mucosa. Eur. J. Biochem., 118: 565-569, 1981.

Reilly RT, Foresthoefel AM, Berger FG. Functional effects of amino acid substitutions at residue 33 of human thymidylate synthase. Archives of Biochemistry and Biophysics, 342(2): 338-343, 1997.

Reyes P, Guganig ME. Studies on a Pyrimidine Phosphoribosyltransferase from Murine Leukemia P1534J. J. Biological Chemistry, 250(13): 5097-5108, 1975.

Roos G, Stenram U. Incorporation of 5-Fluorouracil Into Hepatoma and Normal Tissue RNA at Protein Depletion in the Rat. J. Surgical Oncology, 65: 155-158, 1997.

Rosksoski, Robert. Biochemistry. Philadelphia, Pennsylvania: W.B. Saunders Company, 1996.

Rustum YM, Harstrick A, Cao S, Vanhoefer U, Yin M, Wilke H, Seeber S. Thymidylate synthase inhibitors in cancer therapy: direct and indirect inhibitors. J. Clinical Oncology, 15(1): 389-400, 1997.

Schumacher HJ, Wilson JG, Jordan RL. Potentiation of the Teratogenic effects of 5-fluorouracil by natural pyrimidines. Teratology, 2(2): 99-105, 1969.

Schwartz PM, Moir RD, Hyde CM, Turek PJ, Handschumacher RE. Role of uridine phosphorylase in the anabolism of 5-fluorouracil. Biochemical Pharmacology, 34(19): 3585-3589, 1985.

Schwartz PM, Turek PJ, Hyde CM, Cadman EC, Handschumacher RE. Altered Plasma Kinetics of 5-FU at high dosage in Rat and Man. Cancer Treat. Rep., 69: 133-136, 1985.

Setzer RW, Lau C, Mole ML, Copeland FM, Rogers JM, Kavlock RJ. Toward a Biologically Based Dose-Response Model for Developmental Toxicity of 5-Fluorouracil in the Rat: Modeling Nucleotide pool perturbations. Unpublished.

Shuey DL, Buckalew AR, Wilke TS, Rogers JM, Abbott BD. Early events following maternal exposure to 5-fluorouracil lead to dysmorphology in cultured embryonic tissues. Teratology, 50: 379-386, 1994.

Shuey D, Lau C, Logsdon T, Zucker R, Elstein K, Narotsky M, Setzer W, Kavlock R, Rogers J. Biologically-based dose-response modeling in developmental toxicology: biochemical and cellular sequelae of 5-fluorouracil exposure in the developing rat. Toxicology and Applied Pharmacology, 126: 129-144, 1994.

Shuey D, Zucker R, Elstein K, Rogers J. Fetal anemia following maternal exposure to 5-fluorouracil in the rat. Teratology, 49: 311-319, 1994.

Stevens AN, Morris PG, Iles RA, Sheldon PW, Griffiths JR. 5-FU metabolism monitored *in vivo* by ^{19}F NMR. Br. J. Cancer, 50: 113-117, 1984.

Tateishi T, Matanabe M, Nakura H, Tanaka M, Kumai T, Kobayashi S. Sex- or age-related differences were not detected in the activity of dihydropyrimidine dehydrogenase from rat liver. Pharmacological Research. 35(2): 103-106, 1997.

TOXNET. Toxnet.nlm.nih.gov/servlets/simple-search.

van der Wilt CL, van Groeningen CJ, Pinedo HM, Smid K, Hoekman K, Meijer S, Peters G. 5-fluorouracil/leucovorin-induced inhibition of thymidylate synthase in normal tissue of mouse and man. J. Cancer Res. Clin. Oncol., 123: 595-601, 1997.

Wilson JG. Use of rhesus monkeys in teratological studies. Federation Proceedings, 30(1): 104-109, 1971.

Wilson JG, Jordan RL, Schumacher H. Potentiation of the teratogenic effects of 5-fluorouracil by natural pyrimidines. Teratology, 2(2):91-97, 1969.

Zhang R, Liu T, Soong S-J, Diasio RB. A Mathematical Model of the Kinetics and Tissue Distribution of 2-fluoro-β-alanine, the major Catabolite of 5-fluorouracil. Biochemical Pharmacology, 45(10): 2063-2069, 1993.

Zhang R, Soong S-J, Liu T, Barnes S, Diasio RB. Pharmacokinetics and Tissue Distribution of 2-fluoro-β-alanine in rats. Drug Metabolism and Disposition, 20(1): 113-119, 1992.